Photo-Fenton-like degradation of bisphenol A by persulfate and solar irradiation

Marina Khandarkhaeva[1,2], Agniya Batoeva*[1], Marina Sizykh[1], Denis Aseev[1], Natalia Garkusheva[1]

[1] Baikal Institute of Nature Management of Siberian Branch of the Russian Academy of Sciences, 6, Sakhyanova St., Ulan-Ude 670047, Russia

[2] Okinawa Institute of Science and Technology, 1919-1 Tancha, Onna-son, Okinawa-ken, Japan 904-0495

E-mail: abat@binm.ru

This work evaluates the feasibility of a solar-enhanced Fenton-like process using $S_2O_8^{2-}$ (PS) and Fe^{2+} for the elimination of BPA, a model endocrine-disruption compound. This comparative study of BPA removal showed that among the approaches employed, the effectiveness of BPA degradation (10 mg/L) decreased in the order: Solar/PS/ Fe^{2+}> Solar/PS > PS/ Fe^{2+}> Solar/Fe^{2+}> Solar. The complete degradation of BPA was achieved by Solar/PS/ Fe^{2+} treatment at a [PS]:[BPA] ratio of 20 in less than t_{30W} 5 in deionised water. The high efficiency of the Solar/PS/Fe^{2+} process revealed a synergistic effect (φ = 2.38) between the applied activation agents on the formation of reactive oxygen species (ROS) and subsequent decomposition of BPA. The treatment was accompanied by total organic carbon (TOC) removal (44%) in 45 min. Sequential generation of reactive oxygen species has made Solar/PS/ Fe^{2+} a kinetically effective process for removing BPA without accumulation of toxic intermediates. The reaction rate followed pseudo-first-order kinetics that increased with increasing PS and Fe^{2+} concentrations. Experimental evidence suggests that exposure to solar irradiation maintains suitable quantities of free Fe^{2+} in the reaction mixture, even at low catalyst concentrations (the molar ratio of [PS]:[Fe^{2+}] varied from 0.01 to 0.08). The effects of HCO_3^-, SO_4^{2-}, and Cl^- were also examined. As expected, HCO_3^- and SO_4^{2-} inhibited BPA oxidation. The effect of Cl^- on the oxidation efficiency of BPA in Fenton-like systems depends not only on actual Cl^- concentrations but it is also highly influenced by molar ratios of Cl^- to oxidant and catalyst. Inhibition, which was caused by Cl^- in the mM range can be overcome by prolonging the reaction time or increasing the initial Fe^{2+}concentration.

Finally, the efficiency of Solar/PS/Fe^{2+} process was examined in diluted natural surface water and wastewater effluent. On eliminating the buffering action of HCO_3^-/CO_3^{2-} ions by lowering the pH value to 4.5, complete BPA degradation was achieved in all real water matrices.

Keywords: bisphenol A, persulfate, solar- enhanced Fenton-like process, water matrix

Introduction

Bisphenol A (BPA) is widely used for producing polycarbonate, polyvinyl chloride, epoxy and other resins (Yang et al., 2018). The presence of BPA, an endocrine disrupting compound, has raised public concern as it is frequently found in municipal wastewater, landfill leachate, and even in natural rivers (Dupuis et al., 2012; Seachrist et al., 2016; Torres et al., 2015). Conventional processes are not able to completely remove BPA from aquatic environments as BPA is highly resistant to biological and chemical degradation (Bertanza et al., 2011; Hu et al., 2007; Press-Kristensen et al., 2008).

Various techniques have been proposed to remove BPA from wastewater, including membrane separation (Muhamad et al., 2016; Pan et al., 2019), adsorption (Bhatnagar and Anastopoulos, 2017; Ahamad et al., 2019), biocatalytic membrane processes (Li et al., 2018; Cao et al., 2016; Yang et al., 2013), photo-catalytic oxidation (Dhiman et al., 2017; Al-Kahtani et al., 2019; Huang et al., 2015; Huang et al., 2016; Huang et al., 2017), advanced oxidation processes (Wardenier et al., 2019; Xiao et al., 2017; Moreira et al., 2017).

In recent years, sulfate radical-based advanced oxidation processes (SR-AOPs) have proven to be effective for removal of organic pollutants such as *tert*-buthylmethylether, chlorinated ethenes, pharmaceuticals, etc. (Matzek and Carter, 2016; Wacławek et al., 2017; Guerra-Rodríguez et al., 2018). Sulfate anion radical $SO_4^{\bullet-}$ can be generated *in situ* after activation of persulfate $S_2O_8^{2-}$ (PS) or peroxymonosulfate HSO_5^-(PMS). Among activation methods, application of transition metal ions, especially ferrous iron (Fe^{2+}), offers high efficiency despite low energy demands. Worthy noting is that iron is environmentally friendly, relatively nontoxic and cost effective in comparison with other options.

As in the classical Fenton reaction, Fe^{2+} reacts with PS to form $SO_4^{\bullet-}$ (Eq.1)(Fordham and Williams, 1951).

$$Fe^{2+} + S_2O_8^{2-} \rightarrow SO_4^{\bullet-} + SO_4^{2-} + Fe^{3+} \qquad k = 17 - 20 \quad M^{-1}\,s^{-1} \qquad (1)$$

$$Fe^{3+} + S_2O_8^{2-} \rightarrow 2\,SO_4^{\bullet-} + Fe^{2+} \qquad k = 22.5 - 33.5\ M^{-1}\,min^{-1} \qquad (2)$$

The resulting Fe^{3+} can be reduced back to Fe^{2+} by a second molecule of PS; however, the reduction (Eq.2) is much slower than the initial step (Eq.1) and constitutes the rate-limiting step of the reaction. By immobilizing the active phase on a suitable support (i.e. activated carbon, zeolites, alumina etc.) and using various heterogeneous catalysts, it has been attempted to overcome the rate-limiting step. However, synthesis of such catalysts is complex, expensive and can increase the wastewater stream, produced during their fabrication. Another approach, that considerably improves the degradation rate of contaminants in the homogeneous Fe^{2+}/PS system, is irradiation (Brienza and Katsoyiannis, 2017; Sizykh et al., 2018). Solar irradiation is especially

attractive, because it offers a potentially low-cost, efficient, and environmentally safe hybrid AOPs (Klamerth et al., 2010; Wang et al., 2017; Garkusheva et al., 2017). The effect of irradiation is the photoreduction of ferric ion complexes, e.g. Fe(III)-hydroxo complex $[Fe(OH)(H_2O)_5]^{2+}$ and Fe(III)-coordinated organic ligands $[Fe(OOC–R)]^{2+}$, which regenerate Fe^{2+} via ligand-to-metal charge-transfer reactions (Eqs.3-5) (Evans and Uri, 1949; Pozdnyakov et al., 2000; Tang et al., 2012). The reactions also produce additional radical species, responsible for propagation of radical chain mechanisms. Moreover, ultraviolrt (UV) light can directly excite organic contaminant molecules, leading to their photochemical destruction.

$$[Fe(OH)(H_2O)_5]^{2+} + H_2O \xrightarrow{h\nu} [Fe(H_2O)_6]^{2+} + HO^{\bullet} \ (< \text{ca. } 410 \text{ nm}) \quad (3)$$

$$Fe^{3+} + H_2O \xrightarrow{h\nu} Fe^{2+} + HO^{\bullet} + H^{+} \quad (4)$$

$$[Fe(OOC–R)]^{2+} \xrightarrow{h\nu} Fe^{2+} + R^{\bullet} + CO_2 \quad (< \text{ca. } 500 \text{ nm}) \quad (5)$$

Several studies have examined photo-Fenton(-like) processes for degradation of organic compounds such as perfluorooctanoic acid (Tang et al., 2012), pharmaceutical residues (Paiva et al., 2018), etc. Particularly, Molkenthin et al. (2013) studied UV-A, UV-C, and visible-light assisted Fenton-like treatment of BPA. Complete BPA (50 mg/L) and significant DOC removal in deionised water (H_2O_2:Fe^{2+}:BPA = 23:0.5:1 and pH5) was achieved in 3 and 90 min, respectively. Ahmed and Chiron showed that sequential generation of $SO_4^{\bullet-}$ and $HO^{\bullet}$, occurring during PS/Fe^{2+} treatment under simulated sunlight irradiation (1500W Xe lamp, λ>290nm), facilitated complete mineralization of carbamazepine (CBZ 50 µg/L) from domestic wastewater in 30 min without accumulation of toxic intermediates (1500W Xe lamp, λ>290nm, pH3, molar PS:Fe^{2+}:CBZ ratio of 40:20:1) (Mahdi Ahmed and Chiron, 2013). In a comparative study, Brienza et al. (–2014) demonstrated ~~that~~ better kinetic results for the removal of 17β-estradiol from secondary treated wastewater effluent by solar-assisted PMS/Fe^{2+} than those obtained for solar photo-Fenton (Solar/H_2O_2/Fe^{2+}) and heterogeneous photocatalysis using titanium dioxide (Solar/TiO_2).

Although SR-AOPs have been gaining interest, the number of studies utilizing solar-assisted catalytic processes remains still limited. This study deals with BPA oxidation by a solar-assisted Fenton-like process involving PS and ferrous ion. The present research aimed at examining not only the treatment performance, but also at studying the influence of inorganic anions like bicarbonate (HCO_3^-), chloride (Cl^-) and sulfate (SO_4^{2-}) on the degradation rate of a target contaminant. Finally, experiments were also conducted in raw freshwater spiked with BPA to elucidate the treatability and detoxification behavior of BPA in real water matrices. To the best of our knowledge, this is the first application of the Solar/PS/Fe^{2+} process for degrading BPA in the model aqueous solution as well as in synthetic and real water.

1. Materials and Methods

1.1. Chemicals

BPA (≥99%, Sigma Aldrich, USA), potassium persulfate $K_2S_2O_8$, iron (II) sulfate $Fe_2SO_4 \cdot 7H_2O$, NaCl, Na_2SO_4, HPLC-grade acetic acid, and $NaHCO_3$ ("Khimreaktivsnab", Russia) were used as received. HPLC-grade acetonitrile was purchased from Cryochrom (Russia). Stock solutions were prepared using Milli Q water (18.2 mΩ cm, produced with a Simplicity®UV system from Millipore (USA)).

1.2. Water matrices

Natural surface water was collected from Lake Baikal (**SW1**), Lake Gusinoye (**SW2**) and the Selenga river (**SW3**). Treated municipal wastewater secondary effluent (**TWW**) was obtained from the municipal wastewater treatment plant at Ulan-Ude (Russia). Water samples were filtered the same day (0.2 μm NC, Vladisart, Russia) and stored at 4°C until experiments were performed. DOC levels in the SW1, SW2, SW3 and TWW were 1.51, 4.32, 7.13 and 14.43 mg/L, respectively. The water samples SW2, SW3, and TWW were diluted by ~ 3, 5 and 10 times in order to have the same DOC as in SW1 (1.51 mg/L). This allowed for a more direct investigation of the effect of dissolved organic matter (DOM). Table S1 summarizes the water quality data after dilution.

1.3. Experimental procedure

Experiments were performed in both synthetic solutions (using deionised water (DW)) for fundamental investigations and in natural matrices for simulating water treatment conditions. The initial BPA concentration of 10 mg/L was selected for degradation experiments, because it is an appropriate concentration to accurately follow and calculate BPA kinetics as well as to measure TOC removal and acute toxicity. It was also reported that BPA concentration in "mg/L" range occurred in some wastewater and landfill leachate (Yamamoto et al., 2001; Aziz et al., 2018).

In the first set of the experiments, BPA was subjected to the following treatments:

- sunlight exposure (**Solar**)
- dark Fenton-like process (**PS/Fe^{2+}**)
- PS and sunlight exposure (**Solar/PS**)
- Fenton-like process with sunlight exposure (**Solar/PS/Fe^{2+}**).

Dark (control) experiments with PS were also conducted, but no noticeable degradation of BPA was observed. This is attributed to the fact that PS itself is a mild oxidant; therefore, these results

were not further discussed. A second set of experiments in water matricies, using the Solar/PS /Fe^{2+} system was conducted at an initial pH of 7.5 (without pH pre-adjustment), and pH of 4.5 (corrected by sulfuric acid) to eliminate the buffer action of HCO_3^-/CO_3^{2-}.

Experiments were conducted under natural sunlight in summer (N51°48'47.747", E107°7'19.536"). Solar radiation intensity in UV and visible range was measured using a UV-radiometer TKA-PKM (TKA Scientific Instruments, Russia). The principal scheme of the experimental unit has been previously described (Khandarkhaeva et al., 2017). The flow rate of the treated solution was 1 L min^{-1} and the total volume was 1 L. Experiments were conducted without external temperature control in unbuffered pH conditions. During the course of the reactions, changes in temperature and pH were monitored. An appropriate amount of oxidant was added to a BPA-containing reaction solution (1 L. The reaction was initiated on adding the freshly prepared Fe^{2+} catalyst solution (1 mg/mL) and simultaneous starting solar irradiation. Dark experiments were conducted without exposure to sunlight. Samples were taken at regular intervals with total run time of 120 min. In order to stop the Photo-Fenton-like reaction, prior to HPLC analysis of residual BPA, pH of the collected samples were immediately adjusted to pH 7.5-8.0 with 1 N NaOH. This allows ferric iron to precipitate ~~out~~ as ~~an~~ insoluble and amorphous ferric hydroxide. 0.45 µm PTFE membrane filters (Vladisart, Russia) were used to remove the ferric hydroxide flocs. $NaNO_2$ was used to quench radical reactions for TOC analysis. All experiments were performed in duplicates.

1.4. Data presentation

"Normalized illumination time" $t_{30W,n}$ (Table S2) was used in calculations of kinetic parameters (Hincapie et al., 2005; Jiménez et al., 2011; Malato et al., 2009), such that results obtained on different days (under different solar irradiation conditions) can be compared. This normalizes results to a solar UV irradiance of 30 W/m^2, a typical solar UV irradiance on a sunny day. This is calculated by the equation

$$t_{30W,n} = t_{30W,n-1} + \Delta t_n \times \frac{UV}{30}\frac{V_i}{V_t}, \qquad \Delta t_n = t_n - t_{n-1}$$

where t_n is the experimental time for each sample (min), V_i is the illuminated volume (0.416 L), V_t is the total volume of the photoreactor (1 L), and UV is the average solar UV irradiation measured during Δt_n (W m^{-2}).

1.5.Analytical methods

Changes in the BPA concentration during treatment were measured with an Agilent 1260 Infinity HPLC-FLD using a Zorbax SB-C18 column (4.6 x 150 mm with a 5 µm particle size) at 228 nm. A 45:55 mixture of acetonitrile and 75 mM acetic acid was used for the mobile phase. A 0.5 mL/min flow rate and 50 µL sample volume at 35°C was used. The excitation and emission

wavelengths were 230 and 315 nm, respectively. Changes in TOC content as measured by a Shimadzu TOC-L CSN (detection limit 50 μg L^{-1}) were used to assess the degree of BPA mineralization. For TOC analyses, potassium hydrogen phthalate and sodium bicarbonate solutions were used as the calibration standards. Oxidation efficiency and mineralization of dissolved organic compounds were assessed by BPA conversion and TOC removal, according to the equation

$$E(\%) = \left(1 - \frac{C_\tau}{C_0}\right) \times 100\,,$$

where C_0 and C_τ are the concentrations of BPA (or TOC) initially and after treatment time τ (min). Synergistic index was calculated as:

$$\varphi = \frac{E_{(\mathrm{Solar/\,PS/Fe^{2+}})}}{E_{(\mathrm{Solar/\,PS})} + E_{(\mathrm{PS/Fe^{2+}})}},$$

where E_n – oxidation efficiency (E, %) in 5 min.

Absorption spectra of ~~the~~ solutions were recorded using an Agilent UV-VIS 8453 spectrophotometer with a quartz cuvette (1-cm path length). Toxicity of treated and unfiltered samples after quenching of residual oxidant with $NaNO_2$, was assessed using a Biotox 10M toxicity assessment kit, based on luminescence of a recombinant strain of *E. coli* K12 TG1 carrying a lux operon of the luminescent bacterium, *Photobacterium leiognathi (For more details see Supplementary Material, Text A*).

2. Results and Discussion

2.1. A comparative study

At first, control experiments for BPA removal were carried out using different processes (Solar, Solar /PS, PS/Fe^{2+}, Solar/PS/Fe^{2+}) under the same conditions (Fig. 1). Experiments under solar irradiation without any oxidant or catalyst showed that BPA removal was insignificant (3 %). The BPA absorption spectrum exhibited absorption maxima at 228 and 280 nm, implying that the amount of solar irradiation in the UV-C range was not capable of inducing electron state transitions that transform BPA. Several previous studies have also demonstrated BPA's limited capacity to absorb light even in the UV-C range (Rosenfeldt and Linden, 2004; Rivas et al., 2009). Neamtu and Frimmel (2007) reported only 25% removal of BPA after 120 min irradiation with a low-pressure Hg lamp (15 W, an incident photonic flux of 4.25×10^{-6} Einstein s^{-1}). In the current study, combination of solar irradiation and PS remarkably enhanced the efficiency of BPA degradation, compared to photolysis alone; BPA was completely removed in t_{30W} = 45 min. The result can be explained as follows: activated PS decomposes following the Haber-Weiss radical chain mechanism, where homolytic cleavage of the O – O bond yields $SO_4^{\bullet -}$ radicals (Eq. 6):

$$S_2O_8^{2-} \xrightarrow{h\nu} 2\ SO_4^{\bullet -} \qquad (6)$$

Addition of exogenic oxidants, such as peroxocompounds, often significantly reduces the UV dose required for oxidation, compared to direct photolysis, enhancing process yields. For instance, Rosenfeldt and Linden (2004) studied BPA destruction by monochromatic low-pressure (254 nm) and polychromatic medium-pressure (200-300 nm) mercury UV lamps; finding a 3% and 15% reduction by direct photolysis. The same samples were then exposed to UV/H_2O_2, which enhanced BPA degradation by up to 90% while estrogenic activity was reduced by nearly 100%, despite the UV source. In the current study, during the initial stage of oxidation, the reaction rate constant k_{app} and half-life $\tau_{1/2}$ were 0.0193 min^{-1} ($R^2 = 0.94$) and 36 min, respectively. After t_{30W} 30 min of treatment, a slight sharp decrease of BPA was observed. It has been previously shown, that even at a modest temperature of 40°C PS can be slowly activated for degrading BPA (Olmez-Hanci et al., 2013; Potakis et al., 2016). According to Olmez-Hanci et al.(2013), 26% of the initial BPA concentration (20 mg/L) was removed at a [PS]:[BPA] molar ratio of 114:1 at 40°C after 120 min. In our experiments, spontaneous heating of the reaction mixture was observed (up to 38 - 40°C) during the treatment. It was hypothesised, that temperature may also contribute to BPA removal through heat decomposition of PS at the final oxidation stage. (Eq.6). Thus, co-activation of PS by both solar-irradiation and by temperature in the solar/$S_2O_8^{2-}$ process might occur. However, BPA elimination still occurred slowly, as PS only absorbs light at $\lambda < 320$ nm (Anipsitakis and Dionysiou, 2004) and PS decomposition by heat requires high activation energy (184±12 kJ/mol) (Olmez-Hanci et al., 2013). Comparatively rapid BPA elimination in the first few minutes of treatment with PS/Fe^{2+} was achieved, reaching a plateau quickly (2-3 min). The high initial rate demonstrates that PS molecules decomposed effectively in the presence of ferrous ions compared to solar irradiation. PS reacts with Fe^{2+} to produce $SO_4^{\bullet-}$ followed by elimination of BPA by the $SO_4^{\bullet-}$ (Eq.1). However, a quick release of active radicals may not necessarily increase oxidation efficiency. When Fe^{2+} was fully oxidized to Fe^{3+} a plateau was reached, resulting in only 40% BPA elimination, even after prolonged reaction times. As discussed above, the slow regeneration rate of Fe^{2+} (Eq.2) limits oxidation efficiency PS/Fe^{2+}, while Fe^{3+} cannot activate PS in the dark (Liang et al., 2009). Moreover, scavenging of excess $SO_4^{\bullet-}$ during the initial stage is highly likely according to the following reactions (Kusic et al., 2011; Clifton and Huie, 1989; Buxton et al., 1999) ~~[36-38]~~:

$$SO_4^{\bullet-} + Fe^{2+} \rightarrow SO_4^{2-} + Fe^{3+} \qquad k = 4.6 \times 10^9\ M^{-1}s^{-1} \tag{7}$$

$$SO_4^{\bullet-} + SO_4^{\bullet-} \rightarrow S_2O_8^{2-} \qquad k = 4 \times 10^8\ M^{-1}s^{-1} \tag{8}$$

$$SO_4^{\bullet-} + S_2O_8^{2-} \rightarrow SO_4^{2-} + S_2O_8^{\bullet-} + H^+ \quad k = 6.1 \times 10^5\ M^{-1}s^{-1} \tag{9}$$

Similar results were reported by Oh and Kang (2010). The authors found that degradation of 2,4-dinitrotoluene in a PS/Fe^{2+} system was short lived, removing only 20% of the contaminant. Degradation efficiency increased significantly when PS was coupled with solar irradiation and Fe^{2} (Fig 1a). Complete BPA elimination was reached in less than t_{30W} 5 min. Moreover, at the end of the treatment, significant TOC removal was achieved (44%). This enhancement is related to the presence of both solar irradiation and Fe^{2+}, which together allow for efficient decomposition of PS and regeneration of Fe^{2+}. The high efficiency of the Solar/PS/Fe^{2+} process revealed a synergistic effect (φ = 2.38) between the applied activat agents on the formation of reactive oxygen species (ROS) and subsequent decomposition of BPA. For comparison, Shiraz et al. (2017) reported the synergetic effect of the photo-Fenton hybrid system UV-C/PS/Fe^{2+} on catechol destruction equal to 1.32.

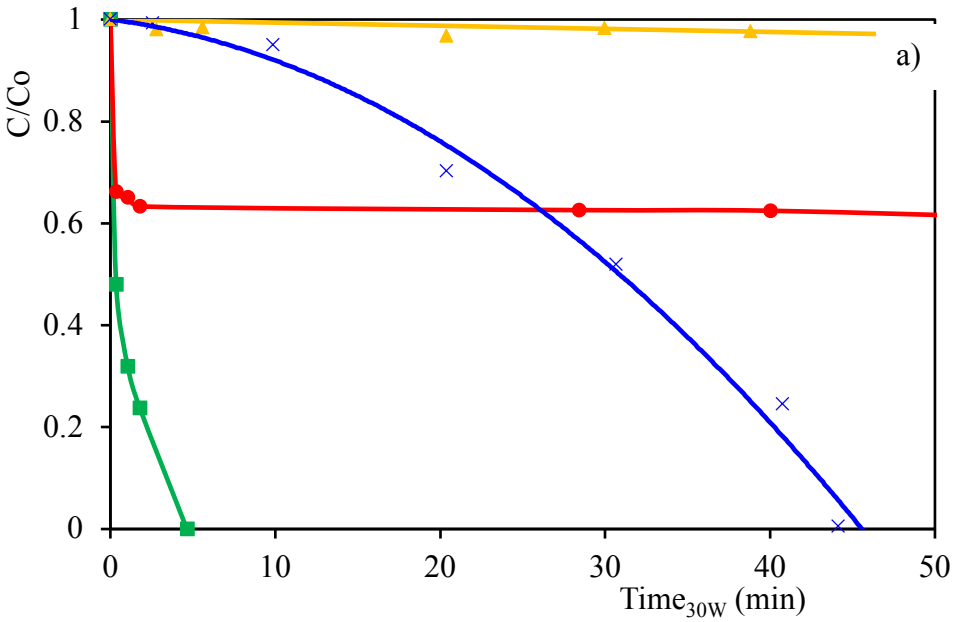

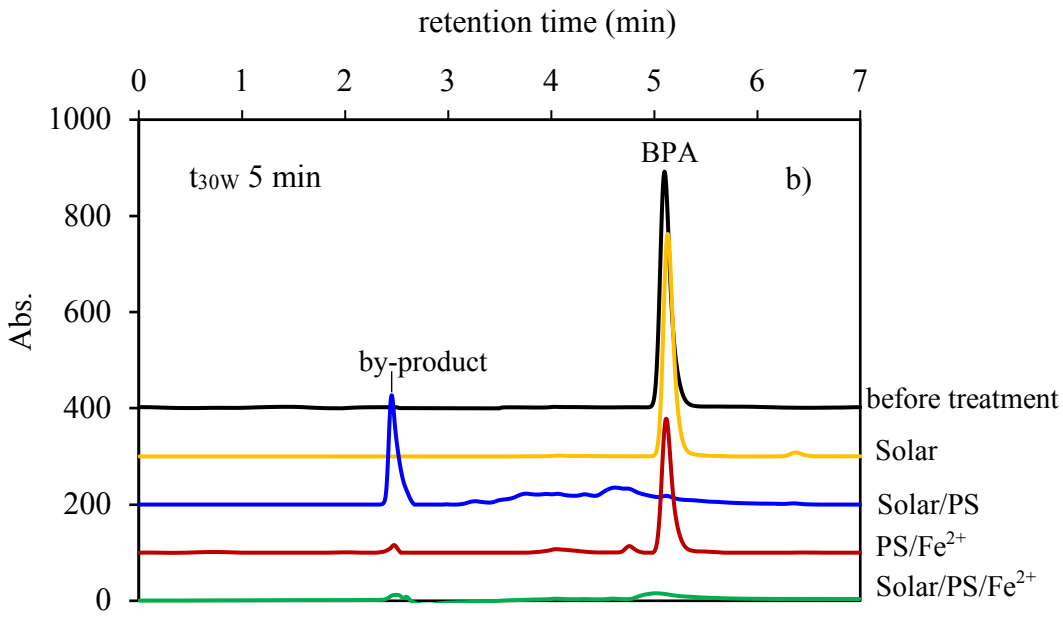

Figure 1. BPA conversion (a) and chromatograms of solutions at λ=228 nm before and after treatment (b) in different oxidative systems; C_0(BPA) =10 mg/L (43.8 μM), [PS]:[BPA] = 20, $C_0(Fe^{2+})$ = 4 mg/L (71.4 μM), t_{30W} = 5 min) recorded at 228 nm pH 5.7.

The decreasing intensity of peaks on the chromatogram after Solar/PS/Fe^{2+} treatment confirms the almost complete disappearance of aromatic compounds (Fig. 1b). Our earlier work (Khandarkhaeva et al., 2017) confirmed that both •OH and $SO_4^{\bullet-}$ radicals were involved in the Solar/PS/Fe^{2+} process. It was proposed that iron-containing hydro-complexes act as photosensitizers in the photochemical oxidation process. Adding iron to the reaction increases the absorbance of the solution and expands the absorption spectrum into the visible region of the solar spectrum (up to 580 nm) (Fig. S1). Under these conditions, ~~the~~ $[Fe(OH)(H_2O)_5]^{2+}$ complex and ferric ion are reduced, which is responsible for regeneration of catalyst and formation of an additional oxidizing species (Huang and Huang, 2009; Molkenthin et al., 2013). This assumption was confirmed experimentally, when exposure to sunlight in the absence of PS (Solar/Fe^{2+}) was tested. Surprisingly, 15 % of BPA was degraded in t_{30W} 40 min, which might be attributed to the involvement of dissolved oxygen in the oxidation process with consequent generation of •OH (Eqs.3,4) (Du et al., 2007; Ya Sychev and G. Isak, 1995; Zhang et al., 2018; Huang et al., 2015; Huang et al., 2016). Recently Pan et al.(Pan et al., 2017) identified colloidal $[Fe(OH)_3]_m$ as an important photoactive Fe(III) species in the degradation of BPA (87% in 16 h). $O_2^{\bullet-}$ is the key active radical (Eqs.10-16).

$$[Fe(OH)_3]_m + 2O_2 \xrightarrow{h\nu} Fe^{2+} + 2O_2^{\bullet-} + H_2O \quad (10)$$

$$O_2^{\bullet-} + Fe^{3+} \rightarrow Fe^{2+} + O_2 \quad (11)$$

$$O_2^{\bullet-} + Fe^{2+} + 2\,H^+ \rightarrow Fe^{3+} + H_2O_2 \quad (12)$$

$$Fe^{2+} + H^+ + H_2O_2 \rightarrow Fe^{3+} + {}^{\bullet}OH + H_2O \quad (13)$$

Additionally, the following reactions may occur (Ermolin et al., 2012):

$$2H^+ + 2\,O_2^{\bullet-} \rightarrow O_2 + H_2O_2 \quad (14)$$

$${}^{\bullet}OH + H_2O_2 \rightarrow HO_2^{\bullet} + H_2O \quad (15)$$

$$Fe^{2+} + OH^{\bullet} \rightarrow Fe^{3+} + OH^- \quad (16)$$

The results underline the importance of dissolved oxygen in iron-catalyzed oxidation. Moreover, in the Solar/PS/Fe^{2+} system, $SO_4^{\bullet-}$ can also react with water to yield ${}^{\bullet}OH$, but the reaction rate constant k is sufficiently low (Eq.17), that this reaction is not a major sink for $SO_4^{\bullet-}$ at TOC > 1 mg/L (Huang and Huang, 2009; Peyton, 1993). At lower TOC values, which occur later in the degradation process, more ${}^{\bullet}OH$ is probably formed.

$$SO_4^{\bullet-} + H_2O \rightarrow SO_4^{2-} + H^+ + {}^{\bullet}OH \quad k = 11.92\ M^{-1}\ s^{-1} \quad (17)$$

Aromatic compounds, which are converted to oxidised molecule fragments and lose their aromaticity, usually exhibit detoxification effects without the need for complete mineralisation. However, early intermediate degradation products can be considerably more toxic than their parent compounds. For example, Gutierrez-Zapata et al. (2017), Olmez-Hanci et al. (2013), Rodríguez et al., (2010) found that toxic intermediates might form during BPA oxidation. To be sure that toxic intermediates (even more toxic than BPA) were not formed, an acute toxicity was assessed for two of the most efficient systems, namely, Solar/PS and Solar/PS /Fe^{2+} (Table 1).

Table 1 Assessment of the acute toxicity index (T_a) of BPA solutions before and after treatment. C(BPA) = 10 mg/L (43.8 μM), [PS]:[BPA] = 20, C(Fe^{2+}) = 4 mg/L (71.4 μM), pH 5.7

Sample	Before			After					
				Solar /PS			Solar/PS/ Fe^{2+}		
	I*, impulses/s		T_a	I*, impulses/s		T_a	I*, impulses/s		T_a
	control	sample		control	sample		control	sample	
1	3664	3087	15.6	3581	1055	69.5	3633	2913	17.0
2	3651	3111	14.8	3942	1089	67.5	3323	3245	5.2
3	3300	2580	20.1	3428	1037	68.7	3245	2624	15.8
Average	16.8±3.4			68.6±3.9			12.7±9.1		

* I – bioluminescence intensity index

The increase of toxicity index (T_a) could be attributed to the formation of more toxic oxidation products in the Solar/PS experiment. At the same time, despite the complete removal of

a parent compound, DOM was not mineralized. We propose the formation of aromatic toxic products in this case, which is confirmed by chromatographic analysis data (Fig. 1b).

In the Solar/PS/Fe^{2+} experiment, i.e., under the activation of persulfate by combining natural solar irradiation and Fe^{2+} ions, the treated water was non-toxic. According to Zazo et al.(2007) and Olmez-Hanci et al.(2013), the subsequent toxicity decrease might be related to benzene ring cleavage in aromatic intermediates with a formation of low toxic organic acids. In our experiments, in integrated Solar/PS/ Fe^{2+} system, along with the complete oxidation of BPA, a quite high mineralization (up to 44%) of DOM has been achieved.

2.2. Effect of Fe^{2+} and PS concentrations

PS

Since the initial concentrations of oxidant and catalyst are known to significant influence the reaction rates of Fenton and other processes, the effect of these parameters on the Solar/PS/Fe^{2+} system was evaluated (Table 2; Fig. S2 - S4). Accordingly, the extent of BPA and TOC degradation increased along with an increasing in the initial concentration of PS over the entire range of [PS]:[BPA] ratios. For instance, at a fixed Fe^{2+} concentration of 1 mg/L (17.86 μM) and at initial [PS]:[BPA] ratio of 5, approximately 62% BPA was eliminated within t_{30W} 5min. When the ratio was increased from 5 to 20, BPA removal reached 83%, while other conditions were identical. At [PS]:[BPA] ratio 36 (36:1 ratio is a stoichiometric requirement, according to a hypothetical reaction (Eq.18)) and at a fixed Fe^{2+} concentration of 4 mg/L (71.4 μM), a significant reduction in the time required for 90% BPA removal $\tau_{90\%}$ was achieved. However, this did not substantially improve TOC removal (~2%).

$$C_{15}H_{16}O_2 + 72\ SO_4^{\bullet-} + 28\ H_2O \rightarrow 15\ CO_2 + 72\ SO_4^{2-} + 72\ H^+ \quad (18)$$

Thus, experimental evidence suggests that a higher [PS]:[BPA] ratio provides more ROS, which contribute to degradation of a target contaminant. At lower ratio of [PS]:[BPA], there was not enough ROS for BPA elimination (Fig.S2, *curve 5:1*). Although, as reported previously, surplus $S_2O_8^{2-}$ can scavenge active radicals (Eqs. 8,9), but this effect was not observed within the investigated concentration range used. Here, a ratio [PS]:[BPA] of 20 was-selected as optimal and was applied to subsequent experiments.

Fe^{2+}

The effect of different Fe^{2+} concentrations on BPA and TOC elimination was investigated in the range of 0.5 - 4 mg/L (8.9 - 71.4 μM). The initial reaction rate (W_0) of BPA oxidation was accelerated on increasing Fe^{2+} concentration (Table 2). The impact of catalyst concentration was especially appreciable at insufficient PS dosages (Fig.S3, [PS]:[BPA] = 5:1).

On increasing PS concentration ([PS]:[BPA] ratio of 20), complete BPA reduction can be achieved within 30 min, irrespective of initial Fe^{2+}concentration (Fig.S3, [PS]:[BPA] = 20:1). However, the degradation rate strongly depended on the Fe^{2+} concentration. The pseudo-first-order reaction rate constants k_{app} were 0.02, 0.40, 0.51 and 1.80 min^{-1} at Fe^{2+} concentrations of 0.5, 1, 2 and 4 mg/L (or 8.9, 17.8, 35.7 and 71.4 μM), respectively. A significant reduction of $\tau_{90\%}$ and high efficiency of BPA destruction at higher iron concentrations are due to higher decomposition rate of PS (Eq.1) with subsequent generation and involvement of ROS in the oxidation process. At the same time, it should be noted that with an increase of initial Fe^{2+} concentration from 1 to 4 mg/L, the degree of mineralization varies slightly - from 39 to 44%. We proposed that larger concentrations of Fe^{2+} (excess) scavenge ROS produced (Eq. 7), therefore, further increasing concentration seemed to be technologically irrelevant.

Experimental evidence suggests that exposure to solar irradiation is capable of maintaining suitable quantities of free Fe^{2+} in reaction mixture, even at low catalyst dosage (molar ration of [PS]:[Fe^{2+}] varied from 0.01 to 0.08). Considering that Fenton and Fenton-like homogeneous systems require iron removal at the end of treatment, the high efficiency of the Solar/PS /Fe^{2+} system even at low catalyst dosage is of practical interest. It might be possible to use naturally occurring iron for micropollutants. For example, a photo-Fenton process has been used to disinfect groundwater (Gutierrez-Zapata et al., 2017).

Table 2 Effect of Fe^{2+} and PS concentrations on BPA degradation; C_0(BPA) =10 mg/L

$C_0(Fe^{2+})$, mg/L	$[S_2O_8^{2-}]$:[BPA]	Oxidation efficiency, %		W_0, μM min^{-1}	$\tau_{90\%}$, min
		BPA elimination*	TOC elimination**		
0	0	2	0	0.31	-
0	20	4	0	0.23	43.0
0.5	5	32	9	11.0	>45
0.5	20	52	32	27.2	19.7
1	5	62	25	32.5	35.5
1	10	65	37	41.6	13.3
1	20	83	39	47.7	6.6
2	5	71	26	30.7	11.0
2	20	90	42	52.0	4.9
4	5	93	27	63.1	5.2
4	20	100	44	65.3	3.4
4	36	100	46	98.1	0.38

* t_{30W} 5 min

** at the end of the treatment

2.3. *Influence of co-existing inorganic anions*

Various ions present in water may affect the efficiency of Fenton and Fenton-like processes (Chaoqun et al., 2013; Matamoros et al., 2008; Moreira et al., 2016). These ions can cause the precipitation of iron scavenging ROS or can coordinate to bind Fe^{3+} and Fe^{2+} into other complexes with higher or lower reactivity (J. Pignatello et al., 2006). Effects of bicarbonate (HCO_3^-), sulfate (SO_4^{2-}) and chloride (Cl^-), the most widely present ions in water, were explored in the present study.

HCO_3^-

Generally, it is assumed that HCO_3^- (CO_3^{2-}) ions significantly limit oxidation efficiency of AOPs because of scavenging $HO^\bullet$ and $SO_4^{\bullet-}$(Chaoqun et al., 2013; Matamoros et al., 2008; Moreira et al., 2016). According to the literature, the detrimental effect of HCO_3^-(CO_3^{2-}) is higher for $HO^\bullet$ compared with $SO_4^{\bullet-}$, because the latter has relatively high selectivity (Huang et al., 2018). In the present study, the effect of HCO_3^- (0 to 100 mg/L) on BPA degradation in the Solar/PS/Fe^{2+} system was evaluated. HCO_3^- negatively impacted BPA degradation efficiency (Fig. 2), a result attributed to the buffering action of HCO_3^-/CO_3^{2-} system. The $pH_{initial}$ and pH_{final} of BPA solutions with 10 - 100 mg/L of $NaHCO_3$ were in the range 6.9-8, which favored precipitation of dissolved iron as hydrous (oxy)hydroxides. While catalyst deactivation is likely to be the main reason for the low efficiency of BPA destruction, competition of HCO_3^- for ROC, i.e. $HO^\bullet$ and $SO_4^{\bullet-}$, should be also considered. Forms of HCO_3^-/CO_3^{2-}in solution are pH dependent. pKa values for the following Eqs. (17,18) are 10.33 and 6.35, respectively. Therefore, in the pH range employed, HCO_3^- was the dominant species, which theoretically could compete for $SO_4^{\bullet-}$ and $HO^\bullet$, according to Eqs. (19,20):

$$HCO_3^- \rightarrow CO_3^- + H^+ \quad (17)$$

$$CO_2 \rightarrow HCO_3^- + H^+ \quad (18)$$

$$HCO_3^- + SO_4^{\bullet-} \rightarrow SO_4^{2-} + HCO_3^{\bullet-} \qquad k = 9.1 \times 10^6\ M^{-1}\ s^{-1} \quad (19)$$

$$HCO_3^- + HO^\bullet \rightarrow CO_3^{\bullet-} + H_2O \qquad k = 8.6 \times 10^6\ M^{-1}\ s^{-1} \quad (20)$$

Thus, at neutral pH, transformation of highly reactive $SO_4^{\bullet-}$ and $HO^\bullet$ to less reactive (hydro)carbonate radicals $HCO_3^{\bullet-}/CO_3^{\bullet-}$ at a relatively fast rate (~10^6 M^{-1} s^{-1}) could reduce overall oxidation strength and inhibit oxidation reactions.

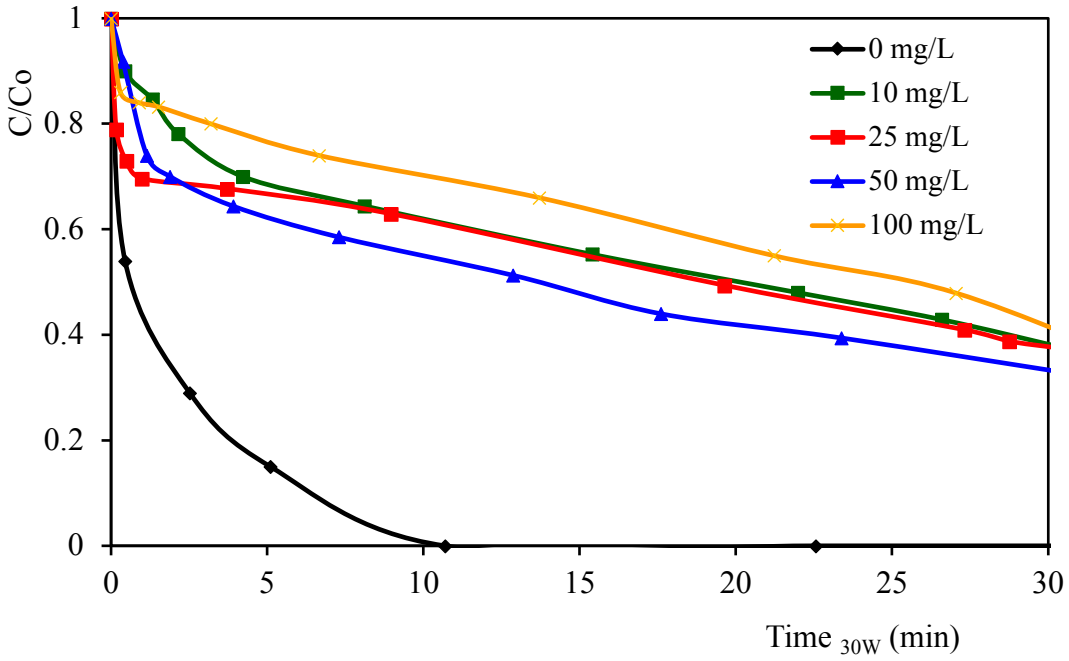

Figure 2. The effect of HCO_3^- on BPA conversion; C_0(BPA) = 10 mg/L (43.8 μM), [$S_2O_8^{2-}$]:[BPA] = 20, $C_0(Fe^{2+})$ = 1 mg/L (17.8 μM)

SO_4^{2-}

In the Solar/PS/Fe^{2+} system, higher SO_4^{2-} concentration (0 to 50 mg/L) resulted in lower k_{app} (Fig.3). The observed results may be explained as follows. Fe^{2+} and Fe^{3+} can rapidly form aqueous complexes with sulphate species:

$$Fe^{2+} + SO_4^{2-} \leftrightarrow FeSO_4 \quad (21)$$

$$Fe^{3+} + SO_4^{2-} \leftrightarrow FeSO_4^+ \quad (22)$$

This decreases the available soluble Fe^{2+} for PS activation. Moreover, the Fe^{2+} reduction (Eq.23), which competes with the Fe(III)-hydroxocomplex, occurs with a very low quantum yield of 1.6 × 10^{-3} and 7.9 × 10^{-3} mol $Einstein^{-1}$ at 350 and 280 nm, respectively (Benkelberg and Warneck, 1995; Machulek et al., 2009).

$$FeSO_4^+ (H_2O)_5 \xrightarrow{h\nu} Fe^{2+}(H_2O)_5 + SO_4^{\bullet-} \quad (23)$$

The $pH_{initial}$ and pH_{final} of BPA solution with added SO_4^{2-} varied from 3.4 - 6.9. Within this pH range, $SO_4^{\bullet-}$ and $HO^{\bullet}$ would both be present in the solution. Previous studies suggested, that SO_4^{2-} does not react with $SO_4^{\bullet-}$ (Ma et al., 2017). In particular, Wang et al. (2016) found that SO_4^- had no impact on the oxidation rate of the herbicide Alachlore by the Fe^0/PS system. A similar result was obtained for BTEX destruction (benzene, toluene, ethhylbenzene and xylenes) by thermally

activated PS (Ma et al., 2017). However, SO_4^{2-} can scavenge $HO^{\bullet}$ via the mechanism in Eq. (22) (Antoniou et al., 2010):

$$HO^{\bullet} + SO_4^{2-}(HSO_4^-) \rightarrow SO_4^{\bullet-}(HSO_4^{\bullet}) + OH^- \quad k = 1.18 \times 10^6\ M^{-1}\ s^{-1} \quad (22)$$

As the pH range was above the second pKa of sulfuric acid (pKa (HSO_4^-/SO_4^{2-}) = 1.92) (Tariq and Yamin, 1998), the dominant species in the solution were SO_4^{2-} ions. The resulting $SO_4^{\bullet-}$ may be scavenged through cannibalization reactions (Eqs.8,9) (Huang et al., 2018; Neta et al., 1988). Similar findings on the detrimental effect of SO_4^{2-} on the efficiency of Fenton-like processes were observed in previous studies (Devi et al., 2013; Devi et al., 2011).

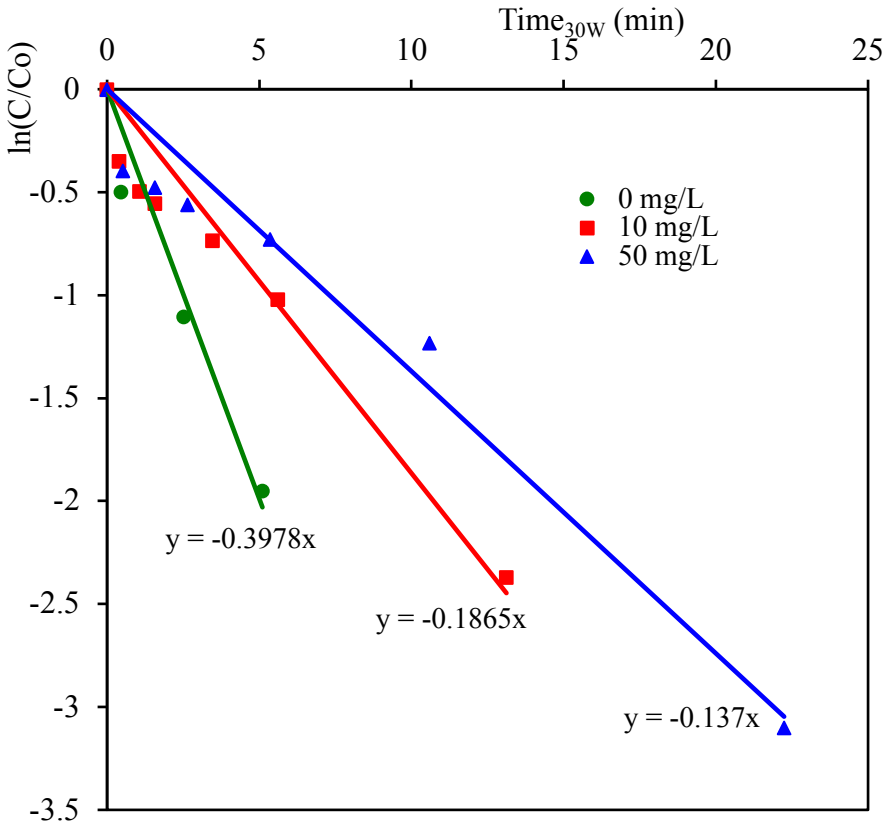

Figure 3. The effect of SO_4^{2-} on BPA conversion; C_0(BPA) = 10 mg/L (43.8 µM), [$S_2O_8^{2-}$]:[BPA] = 20, $C_0(Fe^{2+})$ = 1 mg/L (17.8 µM).

Cl^-

The effect of Cl^- on the oxidation process varies depending on the PS activation method, concentrations, the nature of substrate to be degraded, etc. Accordingly, it is not surprising that both detrimental and beneficial effects of Cl^- on substrate degradation by SR-AOPs have been

reported in previous studies. For instance, the degradation of antipyrene (Chaoqun et al., 2013) and acetic acid (Criquet and Leitner, 2009) by photoactivated PS was promoted in the presence of Cl^- at concentrations below 10 mM. However, when the concentration was further increased, the effect of Cl^- became detrimental. The oxidation of BTEX by thermally activated PS showed that Cl^- inhibited benzene oxidation, while it promoted oxidation of xylenes (Ma et al., 2017). According to our results, Cl^- ions decreased the rate of BPA depletion in the Solar/PS/Fe^{2+} system with [PS]:[Fe^{2+}] = 1:0.02 ($C_0(Fe^{2+})$ =1 mg/L or 17.86 μM) (Fig 4.) Upon the initial addition of Cl (~10 mM), the rate significantly decreased. Further additions however barely affected the reaction rate. The reduction in the oxidation rate can be attributed to the formation of the stable aqua complex of $FeCl^{2+}$ (lgK_1= 3.92) (Laat et al., 2004). The chloro-Fe(III) complex competes with the Fe(III)-hydroxocomplex for UV photons. Hence, the rate of ROS production, i.e. $^{\bullet}OH$, $O_2^{\bullet-}$ and $SO_4^{\bullet-}$ decreases (Eqs.24,25). Initially, the presence of Cl^- did not affect BPA oxidation, since the chloro-Fe(II) complex has a low stability constant (lgK_1= 0.90), and, as was earlier shown with H_2O_2, it has the same reactivity as Fe(II) toward peroxocompounds (Laat et al., 2004; Lu et al., 2005).

Chlorine radicals can influence the Fe(II)/Fe(III) conversion during the catalytic step; reacting directly with Fe^{2+}, based on Eqs (27,28) (Outsiou et al., 2017). This also reduces the concentration of free ferrous ions in the solution which are necessary for the production of $SO_4^{\bullet-}$.

$$Fe^{3+} + Cl^- \leftrightarrow [Fe(Cl)^{2+}] \quad (24)$$

$$[Fe(Cl)^{2+}] \xrightarrow{h\nu} Fe^{2+} + Cl^{\bullet} \quad (25)$$

$$Cl^{\bullet} + Cl^- \leftrightarrow Cl_2^{\bullet-} \qquad k = 2.1 \times 10^{10}\ M^{-1}\ s^{-1} \quad (26)$$

$$k' = 1.1 \times 10^{5}\ M^{-1}\ s^{-1}$$

$$Fe^{2+} + Cl^{\bullet} \rightarrow Fe^{3+} + Cl^- \quad (27)$$

$$Fe^{2+} + Cl_2^{\bullet-} \rightarrow Fe^{3+} + 2Cl^- \quad (28)$$

Moreover, according to the literature, both $^{\bullet}OH$ and $SO_4^{\bullet-}$ can react with Cl^- to form less reactive chlorine species like $Cl^{\bullet}$, $HOCl^{\bullet-}$, $Cl_2^{\bullet-}$, among which, the dichloride anion radical is predominant (Huang et al., 2018) (Eqs.31,32):

$$BPA + SO_4^{\bullet-} \rightarrow \text{intermediate} \qquad k = 4.7 \times 10^{9}\ M^{-1}\ s^{-1} \quad (29)$$

$$BPA + {}^{\bullet}OH \rightarrow \text{intermediate} \qquad k = 8.8 \times 10^{9}\ M^{-1}\ s^{-1} \quad (30)$$

$$^{\bullet}OH + Cl^- \leftrightarrow HOCl^{\bullet-} \qquad k = 4.3 \times 10^{9}\ M^{-1}\ s^{-1} \quad (31)$$

$$k' = 6.1 \times 10^{9}\ M^{-1}\ s^{-1}$$

$$SO_4^{\bullet-} + Cl^- \leftrightarrow Cl^{\bullet} + SO_4^{2-} \qquad k = 2.0 \times 10^{8}\ M^{-1}\ s^{-1} \quad (32)$$

$$k' = 2.5 \times 10^{8}\ M^{-1}\ s^{-1}$$

$$Cl^{\bullet} + Cl^{-} \leftrightarrow Cl_2^{\bullet-} \quad (33)$$

$$BPA + Cl_2^{\bullet-} \rightarrow \text{intermediate} \qquad k = 8.3\times10^{7}\ M^{-1}\ s^{-1} \quad (34)$$

With increasing initial concentration of Fe^{2+} from 1 to 4 mg/L (the ratio of [PS]:[Fe^{2+}] increased from 0.02 to 0.08), the removal rate of BPA was accelerated by the presence of Cl^{-}, compared to controls with no chloride added (Fig. 5). This might be explained as follows: if the rate constant for reverse of Eqs. (31,32) is similar to the forward rate, the reaction may be pushed backwards: thus, having little to no loss of radical oxidation efficiency at moderate Cl^{-} concentrations. The faster degradation of BPA at a ratio [PS]:[Fe^{2+}] = 1:0.08 may be partly attributed to the selective reaction of chlorine radicals with electron-rich BPA. Or another possible influence of Cl^{-} is in decreasing recombination frequency of $SO_4^{\bullet-}$ (Eq.8). This suggests that Cl^{-} cannot be considered as just a ROS scavenger. The effect of Cl^{-} on the oxidation efficiency of BPA in Fenton-like systems depends not only on actual Cl^{-} concentrations but is also highly influenced by molar ratios of Cl^{-} to oxidant and catalyst. Inhibition, which is caused by Cl^{-} in the mM range, can be overcome by prolonging the reaction time or increasing Fe^{2+} initial concentration.

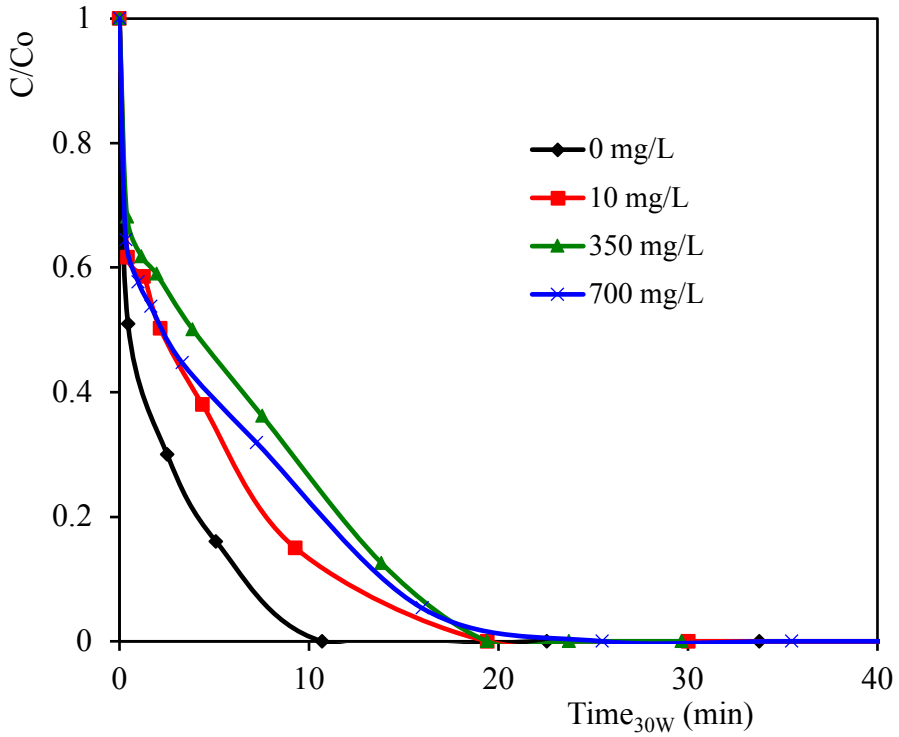

Figure 4. The effect of Cl^{-} on BPA conversion; C_0(BPA) = 10 mg/L (43.8 μM), [$S_2O_8^{2-}$]:[BPA] = 20, C_0(Fe^{2+}) = 1 mg/L (17.8 μM)

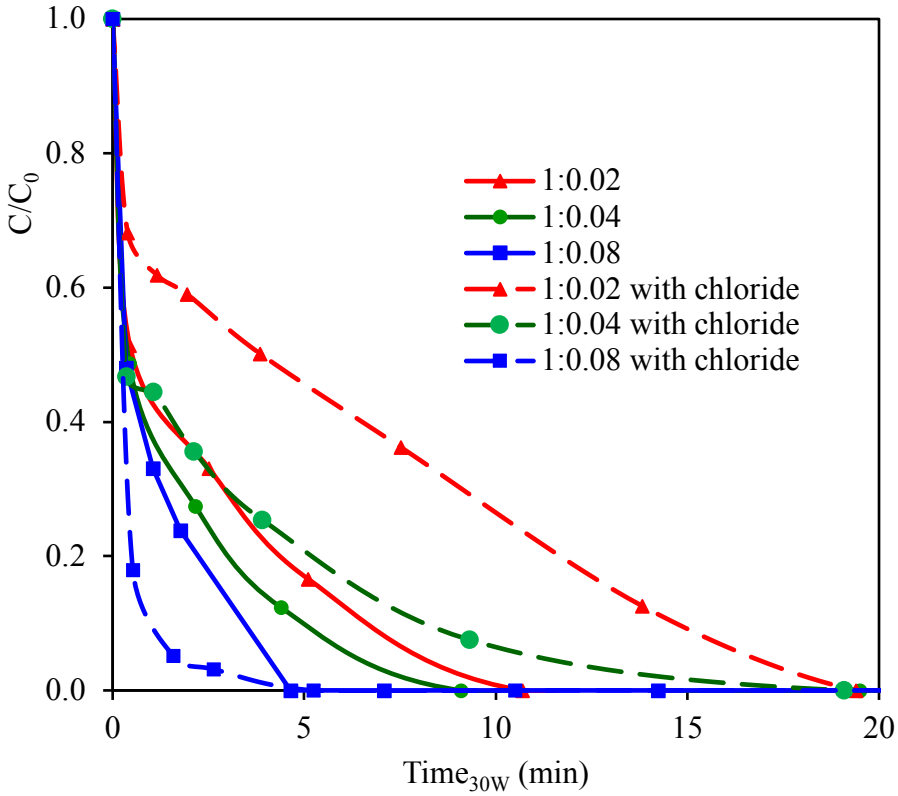

Figure 5. BPA conversion at different initial ratios [PS]:[Fe^{2+}] with (dash) and without (solid) Cl^-; C_0(BPA) = 10 mg/L (43.8 μM), [$S_2O_8^{2-}$]:[BPA] = 20, $C_0(Cl^-)$ = 350 mg/L (9.6 mM)

*1.1.*Influence of water matrix

It is known, that degradation kinetics of a target pollutant and product formation are strongly affected by matrix composition. The matrix typically contains ubiquitous non-target organic and inorganic constituents, which may compete for ROS or incident photons, thus decreasing degradation efficiency. However, there is solid experimental evidence that elimination of target pollutants in real water matrices can be promoted by photochemical reactions, sensitized by the presence of DOM (Canonica et al., 1995; Sokolova and Tchaikovskaya, 2006; Wenk et al., 2011). DOM can form photo-active Fe^{3+} complexes even at neutral and basic pH. Along with soluble Fe^{3+}-organo-complexes, solar irradiation enables the formation of Fe^{2+}, which is required for the catalytic cycle to proceed and form oxidized organocomplexes. Particularly, Peng et al. (2006) found that the presence of algae, humic acids, and Fe(III) favored photodegradation of BPA by UV-A in simulated lake water. In the present study, undiluted SW1 and diluted SW2, SW3, TWW, spiked with 10 mg/L BPA, were sequentially treated by the Solar/PS/Fe^{2+} process at the fixed [PS]:[Fe^{2+}] ratio of 1:0.04. After dilution to 1.5 mg/L DOC, TWW contained Cl^- (0.83 mM) > NO_3^- (0.34 mM) > HCO_3^- (0.21 mM) > NH_4^+ (0.12 mM) > SO_4^{2-} (0.09 mM) ≈ NO_2 > PO_4^{3-},

whereas SWs contained mainly HCO_3^- (0.44 – 98 mM), SO_4^{2-} (0.03 - 0.09 mM) and Cl^- (0.01 - 0.04 mM). Buffering at initial pH (Table S1, pH~7.5) favored precipitation of dissolved iron as hydrous(oxy)hydroxides in all mater matrices. As a result, the Solar/PS/Fe^{2+} process had no benefits for BPA degradation (Fig. S5a). Approximately 25% of BPA load was removed in the few first minutes of treatment, while the remainder continued to decrease at a much slower rate (~ 0.03 min^{-1}), irrespectively of the matrix employed. The slowing down of the BPA oxidation rate in all matrices is primarily due to the deactivation of the catalyst by hydrocarbonates present (13-60 mg/L). pH_{final} were in the range 6.4 - 7.6. The data obtained (Fig. S5a) are in good agreement with the above results on the effect of hydrocarbonates on the process of BPA destruction in the Solar /PS/Fe^{2+} system.

When the buffering action of HCO_3^-/CO_3^{2-} ions was eliminated by lowering the pH to 4.5, accelerated BPA degradation during treatment of all water matrices was observed, but less effectively in TWW (Fig. S5b). The removal rates decreased in the order: SW3~DW>SW2~SW1>TWW (Table 3). Light absorption is minimal at longer wavelengths and increases with decreasing λ, corresponding to the spectra of various humic and fulvic acids (Fig. S6). There were no distinctive absorption bands on spectra of all water matrices, except for the SW3 spectrum with two unidentified peaks at 210 and 260 nm. Absorbance at 260 nm is normally attributed to aromatic hydrocarbons with two or more benzene rings. The maximum BPA elimination in SW3 can be explained by the presence of DOM, which form complexes with iron and iron oxides, promoting Fenton-like oxidation processes (Canonica et al., 1995; Peng et al., 2006). In TWW, the detrimental effect of matrix is likely caused by high content of co-existing inorganic anions and/or light screen effect of DOM.

Table 3. Degradation of BPA by Solar/$S_2O_8^{2-}$/Fe^{2+} processes in aqueous matrices [BPA] = 43.8 μM, [$S_2O_8^{2-}$]:[BPA] = 20:1, [Fe^{2+}] = 35.7 μM.

Matrix	$\tau_{1/2}$, min	$\tau_{90\%}$, min	k, min^{-1}	R^2
DW	0.4	4.9	0.51	0.89
SW1	1.4	9.2	0.25	0.96
SW2	0.8	10	0.26	0.96
SW3	0.4	4.4	0.56	0.97
TWW	4.8	28.2	0.07	0.99

Conclusions

Kinetics of BPA degradation during treatment with a solar-enhanced oxidative system involving ferrous ion (II) and persulfate (PS) were studied. This comparative study of BPA removal showed that among the approaches employed, the order of increasing effectiveness of BPA degradation (10 mg/L) is Solar <Solar/Fe^{2+} <PS/ Fe^{2+} <<Solar/PS <Solar/PS/ Fe^{2+}. The Solar/$S_2O_8^{2-}$/Fe^{2+} system proved to be efficient, fast, and environmentally safe for complete BPA elimination from water, concurrently with significant TOC removal. The reaction rate followed pseudo-first order kinetics that increased with increasing PS and Fe^{2+} concentrations. Experimental evidence suggests that exposure to solar irradiation maintains suitable quantities of free Fe^{2+} in the reaction mixture, even at low catalyst concentrations (the molar ratio of [PS]:[Fe^{2+}] varied from 0.01 to 0.08). At the same time, a significant synergistic effect ($\varphi = 2.38$), which was observed in the solar-enhanced Fenton-like system Solar/PS/Fe^{2+}, was provided via the conjugated radical chain mechanism, involving direct photolysis, combined activation of persulfate by natural solar irradiation and Fe^{2+} ions, leading to generation *in-situ* ROS (primarily, $^{\bullet}OH$ and $SO_4^{\bullet-}$). Moreover, under solar irradiation, the $[Fe(OH)(H_2O)_5]^{2+}$ complex and ferric ion are reduced. This process is responsible for the regeneration of catalyst and formation of additional ROS. Wherein iron compounds act not only as catalysts, but also as sensitizers of photochemical oxidation.

The effect of HCO_3^-, SO_4^{2-} and Cl^- as the most common ions of water matrices, has been also studied. As expected, HCO_3^- and SO_4^{2-} inhibited BPA oxidation. The effect of Cl^- on the oxidation efficiency of BPA in Fenton-like systems depends not only on actual Cl^- concentrations but is also highly influenced by molar ratios of Cl^- to oxidant and catalyst. Inhibition caused by Cl^- in the mM range can be overcome by extending the reaction time or increasing the initial concentration of Fe^{2+}.

The freshwater matrices (DOC 1.5 mg/L, pH~ 7.5) negatively impacted the BPA removal rate due to precipitation of dissolved iron. When the buffering action of HCO_3^-/CO_3^{2-} ions was eliminated by lowering the pH value to 4.5, complete BPA degradation during treatment was achieved within ~ t_{30W} 10 and 40 min of the treatment for SWs and TWW, respectively. Evidently, water matrix composition and reagents concentration are important factors for selecting and applying photo-Fenton-like processes.

Acknowledgement

This work was carried out with support from the Program of Basic Research of BINM SB RAS.

References

Ahamad, T., Naushad, M., Ruksana, Alhabarah, A.N., Alshehri, S.M., 2019. N/S doped highly

porous magnetic carbon aerogel derived from sugarcane bagasse cellulose for the removal of bisphenol-A. Int. J. Biol. Macromol. 132, 1031-1038. https://doi.org/10.1016/j.ijbiomac.2019.04.004

Ahmed, M. M., Chiron, S., 2013. Solar photo-Fenton like using persulphate for carbamazepine removal from domestic wastewater. Water Res. 48, 229-236. https://doi.org/10.1016/j.watres.2013.09.033

Al-Kahtani, A.A., Alshehri, S.M., Naushad, M., Ruksana, Ahamad, T., 2019. Fabrication of highly porous N/S doped carbon embedded with ZnS as highly efficient photocatalyst for degradation of bisphenol. Int. J. Biol. Macromol. 121, 415-423. https://doi.org/10.1016/j.ijbiomac.2018.09.199

Antoniou, M., De la Cruz, A., Dionysiou, D., 2010. Degradation of microcystin-LR using sulfate radicals generated through photolysis, thermolysis and e− transfer mechanisms. Appl. Catal. B. 96, 290–298. https://doi.org/10.1016/j.apcatb.2010.02.013

Anipsitakis, G.P., Dionysiou, D., 2004. Transition metal/UV-based advanced oxidation technologies for water decontamination. Appl. Catal. B. 54, 155-163. https://doi.org/10.1016/j.apcatb.2004.05.025

Aziz, A., Agamuthu, P., Fauziah, S.H., 2018. Removal of bisphenol A and 2,4-Di-tert-butylphenol from landfill leachate using plant- based coagulant. Waste Manage. Res. 36, 975-984. https://doi.org/10.1177/0734242X18790360

Benkelberg, H.-J., Warneck, P., 1995. Photodecomposition of Iron(III) Hydroxo and Sulfato Complexes in Aqueous Solution: Wavelength Dependence of OH and SO_4^- Quantum Yields. J. Phys. Chem. 99, 5214-5221. https://doi.org/10.1021/j100014a049

Bertanza, G., Pedrazzani, R., Grande, M.D., Papa, M., Zambarda, V., Montani, C., Steimberg, N., Mazzoleni, G., Lorenzo, D. Di., 2011. Effect of biological and chemical oxidation on the removal of estrogenic compounds (NP and BPA) from wastewater: An integrated assessment procedure. Water Res. 45, 2473-2484. https://doi.org/https://doi.org/10.1016/j.watres.2011.01.026

Bhatnagar, A., Anastopoulos, I., 2017. Adsorptive removal of bisphenol A (BPA) from aqueous solution: A review. Chemosphere. 168, 885-902. https://doi.org/10.1016/j.chemosphere.2016.10.121

Brienza, M., Katsoyiannis, I., 2017. Sulfate Radical Technologies as Tertiary Treatment for the Removal of Emerging Contaminants from Wastewater. Sustainability 9, 1604. https://doi.org/10.3390/su9091604

Brienza, M., Ahmed, M.M., Escande, A., Scrano, L., Chiron, S., Goetz, V., 2014. Relevance of a

photo-Fenton like technology based on peroxymonosulphate for 17β-estradiol removal from wastewater. Chem. Eng. J. 257, 191-199. https://doi.org/10.1016/j.cej.2014.07.061

Buxton, G. V., Bydder, M., Arthur Salmon, G., 1999. The reactivity of chlorine atoms in aqueous solution Part II.The equilibrium $SO_4^{\bullet-}+Cl^- \leftrightarrow Cl^{\bullet}+SO_4^{2-}$. Phys. Chem. Chem. Phys. 1. 269-273. doi:10.1039/a807808d.

Canonica, S., Jans, U., Stemmler, K., Hoigne, J., 1995. Transformation Kinetics of Phenols in Water: Photosensitization by Dissolved Natural Organic Material and Aromatic Ketones. Environ. Sci. Technol. 29, 1822-1831. https://doi.org/10.1021/es00007a020

Cao, X., Luo, J., Woodley, J.M. , Wan, Y., 2016. Bioinspired multifunctional membrane for aquatic micropollutants removal. ACS Appl. Mater. Interfaces. 8, 30511-30522. https://doi.org/10.1021/acsami.6b10823

Chaoqun, T., Gao, N.-Y., Deng, Y., Zhang, Y., Sui, M., Deng, J., Zhou, S., 2013. Degradation of antipyrine by UV, UV/H_2O_2 and UV/PS. J. Hazard. Mater. 260, 1008-1016. https://doi.org/10.1016/j.jhazmat.2013.06.060

Clifton, C. L., Huie, R.E, 1989. Rate constants for hydrogen abstraction reactions of the sulfate radical, SO_4^-. Alcohols. Int. J. Chem. Kinet. 21, 677-687. doi:10.1002/kin.550210807.

Criquet, J., Leitner, N., 2009. Degradation of acetic acid with sulfate radical generated by persulfate ions photolysis. Chemosphere. 77, 194-200. https://doi.org/10.1016/j.chemosphere.2009.07.040

De Laat, J., Truong Le, G., Legube, B., 2004. A comparative study of the effects of chloride, sulfate and nitrate ions on the rates of decomposition of H_2O_2 and organic compounds by Fe(II)/H_2O_2 and Fe(III)/H_2O_2. Chemosphere. 55, 715-723. https://doi.org/https://doi.org/10.1016/j.chemosphere.2003.11.021

Devi, L.G., Munikrishnappa, C., Nagaraj, B., Rajashekhar, K.E., 2013. Effect of Chloride and Sulfate ions on the Advanced Photo Fenton and Modified Photo Fenton Degradation Process of Alizarin Red S. J. Mol. Catal. A Chem. 374-375, 125-131. https://doi.org/10.1016/j.molcata.2013.03.023

Devi, L.G., Raju, K.S.A., Kumar, S.G., Rajashekhar, K.E., 2011. Photo-degradation of di azo dye Bismarck Brown by advanced photo-Fenton process: Influence of inorganic anions and evaluation of recycling efficiency of iron powder. J. Taiwan Inst. Chem. Eng. 42, 341-349. https://doi.org/10.1016/j.jtice.2010.05.010

Dhiman, P., Naushad, Mu., Batoo, K.M., Kumar, A., Sharma, G., Ghfar, A.A., Kumar, G., Singh, M., 2017. Nano $Fe_xZn_{1-x}O$ as a tuneable and efficient photocatalyst for solar

powered degradation of bisphenol A from aqueous environment J. Cleaner Prod. 165, 1542-1556. https://doi.org/10.1016/j.jclepro.2017.07.245

Du, Y., Zhou, M., Lei, L., 2007. The role of oxygen in the degradation of p-chlorophenol by Fenton system. J. Hazard. Mater. 139, 108-115. https://doi.org/10.1016/j.jhazmat.2006.06.002

Dupuis, A., Migeot, V., Cariot, A., Albouy-Llaty, M., Legube, B., Rabouan, S., 2012. Quantification of bisphenol A, 353-nonylphenol and their chlorinated derivatives in drinking water treatment plants. Environ. Sci. Pollut. Res. 19, 4193-4205. https://doi.org/10.1007/s11356-012-0972-3

Evans, M.G., Uri, N., 1949. The dissociation constant of hydrogen peroxide and the electron affinity of the HO_2 radical. Trans. Faraday Soc. 45, 224-230. https://doi.org/10.1039/TF9494500224

Ermolin, S. V., Ivanova, I.P., Knyazev, D. I., Trofimova, S. V., Piskarev, I.M., 2012. Mechanism of water luminescence upon radiolysis under the effect of background radiation. Russ. J. Phys. Chem. A. 86, 1029-1032. https://doi.org/10.1134/S003602441206009X

Fordham, J.W.L., Williams, H.L., 1951. The Persulfate-Iron(II) Initiator System for Free Radical Polymerizations1. J. Am. Chem. Soc. 73, 4855-4859. https://doi.org/10.1021/ja01154a114

Garkusheva, N., Matafonova, G., Tsenter, I., Beck, S., Batoev, V., Linden, K., 2017. Simultaneous atrazine degradation and E. coli inactivation by simulated solar photo-Fenton-like process using persulfate. J. Environ. Sci. Health, Part A. 52, 849-855. https://doi.org/10.1080/10934529.2017.1312188

Guerra-Rodríguez, S., Rodríguez, E., Singh, D. N., Rodríguez-Chueca, J., 2018. Assessment of Sulfate Radical-Based Advanced Oxidation Processes for Water and Wastewater Treatment: A Review. Water. 10, 1828. https://doi.org/10.3390/w10121828

Gutierrez-Zapata, H., Alvear-Daza, J., Rengifo-Herrera, J., Sanabria, J., 2017. Addition of Hydrogen Peroxide to Groundwater with Natural Iron Induces Water Disinfection by Photo-Fenton at Circumneutral pH and other Photochemical Events. Photochem. Photobiol. 93. 1224-1231. https://doi.org/10.1111/php.12779

Hincapie, M., Maldonado, M., Oller, I., Gernjak, W., Sánchez Pérez, J.A., Martín, M.M., Malato, S., 2005. Solar photocatalytic degradation and detoxification of EU priority substances. Catal. Today. 101, 203-210. https://doi.org/10.1016/j.cattod.2005.03.004

Hu, J.Y., Chen, X., Tao, G., Kekred, K., 2007. Fate of Endocrine Disrupting Compounds in Membrane Bioreactor Systems. Environ. Sci. Technol. 41, 4097-4102. https://doi.org/10.1021/es062695v

Huang, H., Li, X., Wang, J., Dong, F., Chu, P.K., Zhang, T., Zhang, Y., 2015. Anionic Group Self-Doping as a Promising Strategy: Band-Gap Engineering and Multi-Functional Applications of High-Performance CO_3^{2-}-Doped $Bi_2O_2CO_3$. ACS Catal. 57, 4094-4103. https://doi.org/10.1021/acscatal.5b00444

Huang, H., Xiao, K., He, Y., Zhang, T., Dong, F., Du, X., Zhang, Y., 2016. *In situ* assembly of BiOI@$Bi_{12}O_{17}Cl_2$ *p-n* junction: charge induced unique front-lateral surfaces coupling heterostructure with high exposure of BiOI {001} active facets for robust and nonselective photocatalysis. Appl. Catal. B. 199, 75-86. http://dx.doi.org/10.1016/j.apcatb.2016.06.020

Huang, H., Xiao, K., Zhang, T., Dong, F., Zhang, Y., 2017. Rational design on 3D hierarchical bismuth oxyiodides via in situ self-template phase transformation and phase-junction construction for optimizing photocatalysis against diverse contaminants. Appl. Catal., B. 203, 879-888. doi: 10.1016/j.apcatb.2016.10.082

Huang, W., Bianco, A., Brigante, M., Mailhot, G., 2018. UVA-UVB activation of hydrogen peroxide and persulfate for Advanced Oxidation Processes: Efficiency, mechanism and effect of various water constituents. J. Hazard. Mater. 347, 279-287. https://doi.org/10.1016/j.jhazmat.2018.01.006

Huang, Y.-F., Huang, Y.-H., 2009. Identification of produced powerful radicals involved in the mineralization of bisphenol A using a novel UV-$Na_2S_2O_8$/H_2O_2-Fe(II,III) two-stage oxidation process. J. Hazard. Mater. 162, 1211-1216. https://doi.org/10.1016/j.jhazmat.2008.06.008

Jiménez, M., Oller, I., Maldonado, M., Malato, S., Hernandez-Ramírez, A., Zapata, A., Peralta-Hernández, J., 2011. Solar photo-Fenton degradation of herbicides partially dissolved in water. Catal. Today. 161, 214-220. https://doi.org/10.1016/j.cattod.2010.11.080

Khandarkhaeva, M., Batoeva, A., Aseev, D., Sizykh, M., Tsydenova, O., 2017. Oxidation of atrazine in aqueous media by solar- enhanced Fenton-like process involving persulfate and ferrous ion. Ecotoxicol. Environ. Saf. 137, 35-41. https://doi.org/10.1016/j.ecoenv.2016.11.013

Klamerth, N., Malato, S., Maldonado, M.I., Agüera, A., Fernández-Alba, A.R., 2010. Application of Photo-Fenton as a Tertiary Treatment of Emerging Contaminants in Municipal Wastewater. Environ. Sci. Technol. 44, 1792-1798. https://doi.org/10.1021/es903455p

Kusic, H., Peternel, I., Ukić, Š., Koprivanac, N., Bolanča, T., Papic, S., Bozic, A.L., 2011. Modeling of iron activated persulfate oxidation treating reactive azo dye in water matrix. Chem. Eng. J. 172, 109-121. doi:10.1016/j.cej.2011.05.076.

Li, S., Luo, J., Wan, Y., 2018. Regenerable biocatalytic nanofiltration membrane for aquatic micropollutants removal. J. Membr. Sci. 549, 120-128. https://doi.org/10.1016/j.memsci.2017.11.075

Liang, C., Liang, C.-P., Chen, C.-C., 2009. pH dependence of persulfate activation by EDTA/Fe(III) for degradation of trichloroethylene. J. Contam. Hydrol. 106, 173-182. https://doi.org/10.1016/j.jconhyd.2009.02.008

Lu, M.-C., Chang, Y.-F., Chen, I.-M., Huang, Y.-Y., 2005. Effect of chloride ions on the oxidation of aniline by Fenton's reagent. J. Environ. Manag. 75, 177-182. https://doi.org/10.1016/j.jenvman.2004.12.003

Ma, J., Yang, Y., Jiang, X., Xie, Z., Li, X., Chen, C., Chen, H., 2017. Impacts of inorganic anions and natural organic matter on thermally activated persulfate oxidation of BTEX in water. Chemosphere. 190, 296-306. https://doi.org/10.1016/j.chemosphere.2017.09.148

Machulek, A., Ermírio F Moraes, J., Okano, L., A Silvério, C., Quina, F., 2009. Photolysis of ferric ions in the presence of sulfate or chloride ions: Implications for the photo-Fenton process. Photochem. Photobiol. Sci. 8, 985-991. https://doi.org/10.1039/b900553f

Malato, S., Fernandez-Ibanez, P., Maldonado, M., Blanco, J., Gernjak, W., 2009. Decontamination and Disinfection of Water by Solar Photocatalysis: Recent Overview and Trends. Catalysis Today. 147, 1-59. https://doi.org/10.1016/j.cattod.2009.06.018

Matamoros, V., Duhec, A., Albaigés, J., Bayona, J.M., 2008. Photodegradation of Carbamazepine, Ibuprofen, Ketoprofen and 17$α$-Ethinylestradiol in Fresh and Seawater. Water. Air. Soil Pollut. 196, 161-168. https://doi.org/10.1007/s11270-008-9765-1

Matzek, L.W., Carter, K.E., 2016. Activated persulfate for organic chemical degradation: A review. Chemosphere. 151, 178-188. https://doi.org/10.1016/j.chemosphere.2016.02.055

Molkenthin, M., Olmez-Hanci, T., Jekel, M., Arslan-Alaton, I., 2013. Photo-Fenton-like treatment of BPA: Effect of UV light source and water matrix on toxicity and transformation products. Water Res. 47, 5052-5064. https://doi.org/10.1016/j.watres.2013.05.051

Moreira, F., Boaventura, R., Brillas, E., Vilar, V., 2016. Electrochemical advanced oxidation processes: A review on their application to synthetic and real wastewaters. Appl. Catal. B. 202, 217-261. https://doi.org/10.1016/j.apcatb.2016.08.037

Muhamad, M.S., Salim, M.R., Lau, W.J., Yusop, Z., 2016. A review on bisphenol A occurrences, health effects and treatment process via membrane technology for drinking water. Environ. Sci. Pollut. Res. Int. 23, 11549-11567. https://doi.org/10.1007/s11356-016-6357-2

Neamtu, M., Frimmel, F.H., 2007. Degradation of endocrine disrupting bisphenol A by 254 nm irradiation in different water matrices and effect on yeast cells. Water Res. 40, 3745-3750. https://doi.org/10.1016/j.watres.2006.08.019

Neta, P., Huie, R., B. Ross, A., 1988. Rate Constants for Reactions of Inorganic Radicals in Aqueous-Solution. J. Phys. Chem. Ref. Data.17, 1027-1284. https://doi.org/10.1063/1.555808

Oh, S.-Y., Kang, S.-G., 2010. Degradation of 2,4-Dinitrotoluene by Persulfate and Steel Waste Powder. Geosystem Eng. 13, 105-110. https://doi.org/10.1080/12269328.2010.10541316

Olmez-Hanci, T., Arslan-Alaton, I., Genc, B., 2013. Bisphenol A treatment by the hot persulfate process: Oxidation products and acute toxicity. J. Hazard. Mater. 263, 283-290. https://doi.org/10.1016/j.jhazmat.2013.01.032

Outsiou, A., Frontistis, Z., Ribeiro, R., Antonopoulou, M., Konstantinou, I., Silva, A.M.T., Faria, J.L., Gomes, H.T., Mantzavinos, D., 2017. Activation of sodium persulfate by magnetic carbon xerogels (CX/CoFe) for the oxidation of bisphenol A: Process variables effects, matrix effects and reaction pathways. Water Res. 124, 97-107. https://doi.org/10.1016/j.watres.2017.07.046

Paiva, V. A. B., Paniagua, C. E. S., Ricardo, I. A., Gonçalves, B. R., Martins, S. P., Daniel, D., Machado, A.E.H., Trovó, A. G., 2018. Simultaneous degradation of pharmaceuticals by classic and modified photo-Fenton process. J. Environ. Chem. Eng. 6, 1086-1092. https://doi.org/10.1016/j.jece.2018.01.013

Pan, M., Ding, J., Duan, L., Gao, G., 2017. Sunlight-driven photo-transformation of bisphenol A by Fe(III) in aqueous solution: Photochemical activity and mechanistic aspects. Chemosphere 167, 353-359. https://doi.org/10.1016/j.chemosphere.2016.09.144

Pan, Z., Yu, F., Li, L., Song, Ch., Yang, J., Wang, Ch., Pan, Y., Wang, T., 2019. Electrochemical microfiltration treatment of bisphenol A wastewater using coal-based carbon membrane. Sep. Purif. Technol. 227, 115695. https://doi.org/10.1016/j.seppur.2019.115695

Peng, Z., Wu, F., Deng, N., 2006. Photodegradation of bisphenol A in simulated lake water containing algae, humic acid and ferric ions. Environ. Pollut. 144, 840-846. https://doi.org/https://doi.org/10.1016/j.envpol.2006.02.006

Peyton, G. R., 1993. The free-radical chemistry of persulfate-based total organic carbon analyzers. Mar. Chem. 41, 91-103. https://doi.org/10.1016/0304-4203(93)90108-Z

Pignatello, J.J., Oliveros, E., MacKay, A., 2006. Advanced Oxidation Processes for Organic Contaminant Destruction Based on Fenton Reaction and Related Chemistry. Crit. Rev.

Environ. Sci. Technol. 36, 1-84. https://doi.org/10.1080/10643380500326564

Potakis, N., Frontistis, Z., Antonopoulou, M., Konstantinou, I., Mantzavinos, D., 2016. Oxidation of bisphenol A in water by heat-activated persulfate. J. Environ. Manage. 195, 125-132. https://doi.org/10.1016/j.jenvman.2016.05.045

Pozdnyakov, I. P., Glebov, E. M., Plyusnin, V. F., Grivin, V. P., Ivanov, Y. V., Vorobyev, D. Y., Bazhin, N.M., 2000. Hydroxyl radical formation upon photolysis of the $Fe(OH)^{2+}$ complex in aqueous solution, Mendeleev Commun. 10, 185-186. https://doi.org/10.1070/MC2000v010n05ABEH001316

Press-Kristensen, K., Lindblom, E., Schmidt, J.E., Henze, M., 2008. Examining the biodegradation of endocrine disrupting bisphenol A and nonylphenol in WWTPs. Water Sci. Technol. 57, 1253-1256. https://doi.org/10.2166/wst.2008.229

Rivas, F. J., Encinas, Á., Acedo, B., Beltrán, F. J., 2009. Mineralization of bisphenol A by advanced oxidation processes. J. Chem. Technol. Biotechnol. 84, 589-594. https://doi.org/10.1002/jctb.2085

Rodríguez, E.M., Fernández, G., Klamerth, N., Maldonado, M.I., Álvarez, P.M., Malato S., 2010. Efficiency of different solar advanced oxidation processes on the oxidation of bisphenol A in water. Appl. Catal. B. 95, 228-237. https://doi.org/10.1016/j.apcatb.2009.12.027

Rosenfeldt, E. J., Linden, K., 2004. Degradation of Endocrine Disrupting Chemicals Bisphenol A, Ethinyl Estradiol, and Estradiol during UV Photolysis and Advanced Oxidation Processes, Environ. Sci. Technol. 38, 5476–5483. https://doi.org/10.1021/es035413p

Seachrist, D.D., Bonk, K.W., Ho, S.M., Prins, G.S., Soto, A.M., Keri, R.A., 2016. A review of the carcinogenic potential of bisphenol A. Reprod. Toxicol. 59, 167-182. https://doi.org/10.1016/j.reprotox.2015.09.006

Shiraz, D.A., Takdastan, A., Borghei, S.M., 2017. Photo-Fenton like degradation of catechol using persulfate activated by UV and ferrous ions: Influencing operational parameters and feasibility studies. J. Mol. Liq. 249, 463-469. https://doi.org/10.1016/j.molliq.2017.11.045

Sizykh, M., Batoeva, A., Tsydenova, O., 2018. UV-Activated Persulfate Oxidation of Orange III Dye Using KrCl Excilamp. Clean - Soil, Air, Water. 46, 1700187. https://doi.org/10.1002/clen.201700187

Sokolova, I. V, Tchaikovskaya, O.N., 2006. Fluorescence and photochemical properties of humic acids. Atmos. Ocean. Opt. 19, 220-222.

Sychev, A.Y., Isak, V.G., 1995. Iron compounds and the mechanisms of the homogeneous catalysis of the activation of O_2 and H_2O_2 and of the oxidation of organic substrates. Russ.

Chem. Rev. 64, 1105-1129. https://doi.org/10.1070/RC1995v064n12ABEH000195

Tang, H., Xiang, Q., Lei, M., Yan, J., Zhu, L., Zou, J., 2012. Efficient degradation of perfluorooctanoic acid by UV-Fenton process. Chem. Eng. J. 184, 156-162. https://doi.org/10.1016/j.cej.2012.01.020

Tariq, S., Yamin, B., 1998. Chemistry and Chemical Reactivity. By John C. Kotz. Molecules. 3, 141. https://doi.org/10.3390/30400141

Torres, A., Ramirez, C., Romero, J., Guerrero, G., Valenzuela, X., Guarda, A., Galotto, M.J., 2015. Experimental and theoretical study of bisphenol A migration from polycarbonate into regulated EU food simulant. Eur. Food Res. Technol. 240, 335-343. https://doi.org/10.1007/s00217-014-2333-6

Wacławek, S., Lutze, H. V., Grübel, K., Padil, V.V.T., Černík, M., Dionysiou, D.D., 2017. Chemistry of persulfates in water and wastewater treatment: A review. Chem. Eng. J. 330, 44-62. https://doi.org/10.1016/j.cej.2017.07.132

Wang, Q., Shao, Y., Gao, N.-Y., Chu, W., Deng, J., Shen, X., Lu, X., Zhu, Y., Wei, X., 2016. Degradation of alachlor with zero-valent iron activating persulfate oxidation. J. Taiwan Inst. Chem. Eng. 63, 379-385. https://doi.org/10.1016/j.jtice.2016.03.038

Wang, Y., Chen, M., Huang, Q., Cui, Y., Jin, Y., Cui, L., Wen, C., 2017. Experimental study of a solar-driven photo-electrochemical hybrid system for the decolorization of Acid Red 26. Energy Convers. Manag. 150, 775-786. https://doi.org/10.1016/j.enconman.2017.08.047

Wardenier, N., Liu, Z., Nikiforov, A., Van Hulle, S.W.H., Leys, Ch. 2019. Micropollutant elimination by O_3, UV and plasma-based AOPs: An evaluation of treatment and energy costs. Chemosphere. 234, 715-724. https://doi.org/10.1016/j.chemosphere.2019.06.033

Wenk, J., von Gunten, U., Canonica, S., 2011. Effect of Dissolved Organic Matter on the Transformation of Contaminants Induced by Excited Triplet States and the Hydroxyl Radical. Environ. Sci. Technol. 45, 1334-1340. https://doi.org/10.1021/es102212t

Xiao, R., Gao, L., Wei, Z., Spinney, R., Luo, S., Wang, D., Dionysiou, D.D., Tang, C.-J., Yang, W., 2017. Mechanistic insight into degradation of endocrine disrupting chemical by hydroxyl radical: An experimental and theoretical approach. Environ. Pollut. 231, 1446-1452. https://doi.org/10.1016/j.envpol.2017.09.006

Yamamoto, T., Yasuhara, A., Shiraishi, H., Nakasugi, O., 2001. Bisphenol A in hazardous waste landfill leachates. Chemosphere. 42, 415-418. https://doi.org/10.1016/S0045-6535(00)00079-5

Yang, S., Hai, F.I., Nghiem, L.D., Nguyen, L.N., Roddick, F., Price, W.E., 2013. Removal of bisphenol A and diclofenac by a novel fungal membrane bioreactor operated under non-

sterile conditions. Int. Biodeterior. Biodegrad. 85, 483-490. https://doi.org/10.1016/j.ibiod.2013.03.012

Yang, S.-Q., Cui, Y.-H., Liu, Y.-Y., Liu, Z.-Q., Li, X.-Y., 2018. Electrochemical generation of persulfate and its performance on 4-bromophenol treatment. Sep. Purif. Technol. 207, 461-469. https://doi.org/10.1016/j.seppur.2018.06.071

Zazo, J.A., Casas, J.A., Molina, C.B., Quantanilla, A., Rodriguez, J.J., 2007. Evolution of eco-toxicity upon Fenton's oxidation of phenol in water. Environ. Sci. Technol. 41, 7164-7170. https://doi.org/10.1021/es071063l

Zhang, R., Wang, X., Zhou, L., Liu, Z., Crump, D., 2018. The impact of dissolved oxygen on sulfate radical-induced oxidation of organic micro-pollutants: A theoretical study. Water Res. 135, 144-154. https://doi.org/10.1016/j.watres.2018.02.028

Supplementary Material

"Photo-Fenton-like degradation of bisphenol A by persulfate and solar irradiation"

Marina Khandarkhaeva, Agniya Batoeva*, Marina Sizykh, Denis Aseev, Natalia Garkusheva

Baikal Institute of Nature Management of Siberian Branch of the Russian Academy of Sciences, 6, Sakhyanova St., Ulan-Ude 670047, Russia

*Corresponding author's e-mail: abat@binm.ru

TEXT A.

The acute toxicity was assessed by measuring the luminescence inhibition of the recombinant strain of *E. coli* K12 TG1 carrying lux operons of the luminescent *Photobacterium leiognathi* (this is the so-called biosensor Ecolum developed at the Department of Biology of Moscow State University) [Danilov V.S., Zarubina A.P., Eroshnicov G.E., Solov'eva L.N., Kartashev F.V., Zavil'gelsky G.B. (2002) The biolumiscent sensor systems with lux-operons from various species of luminescent bacteria // Moscow Uni. Biol. Sci. Bull., I. 3. PP. 20-24].

The biosensor is a culture of lyophilized cells that need rehydration in distilled water for 30 min before the experiment. After rehydration, the cell bioluminescence becomes sufficiently stable for 3–4 h.

The inhibition of the bacteria's bioluminescence is determined in a static test by mixing a defined amount of a sample with a luminous bacteria suspension in a cuvette. The inhibition of the sample's luminescence is determined in comparison to an uninhibited control solution. The luminescence is measured with the Biotox-10M (Russia), a universal luminometer, suitable for portable use. To obtain reliable data bioluminescence is recorded for control and experimental samples in 3 replications.

Toxicity Index (T) during the time of interaction (30 min) of the biosensor with the sample water is determined the luminometer) according to the formula: $T = 100\ (I_k - I) / I_k$, where I_k and I are the intensity (impulse/s) of luminescence of a control and a sample, respectively.

Based on the value of the toxicity index, samples can be classified as follows:

1. The value of T <20 - the sample is non-toxic;
2. The value of T > 20 but <50 - the sample is toxic;
3. The value of T> 50 - the sample is very toxic.

Table S1 Hydrochemical characteristics of water samples used.

Matrix	**SW1**	**SW2**	**SW3**	**TWW**
pH	7.98	7.68	7.47	7.52
DOC, mg/L	1.51	1.50	1.50	1.50
Conductivity, µS/cm	110.7	68.9	21.3	115.1
NH_4^+, mg/L	<0.05	<0.05	0.05	1.63
Fe total, mg/L	<0.007	<0.007	<0.007	0.015
Cu^{2+}, mg/L	<0.001	0.052	0.001	0.002
HCO_3^-, mg/L	60	30	27	13
CO_3^{2-}, mg/L	<6.0	<6.0	<6.0	<6.0
Br^- mg/L	<0.1	<0.1	<0.1	<0.1
NO_3^-, mg/L	<0.1	0.3	0.2	20.8
NO_2^-, mg/L	<0.1	<0.1	<0.1	2.2
SO_4^{2-}, mg/L	5.94	8.49	2.50	8.42
Cl^-, mg/L	0.53	1.34	0.31	29.36
F^-, mg/L	0.17	0.29	0.05	0.05
PO_4^{2-}, mg/L	<0.1	<0.1	<0.1	2.1
COD, mgO/ L	3	6	2	4

Table S2. The intensity of solar radiation during the experiments

The intensity of solar radiation in the bactericidal ranges, W/m^2			Irradiance, Lx
UV-A (315-400 nm)	UV-B (280-315 nm)	UV-C (200-280 nm)	
22-42	1,7-2,8	2,0-3,2	81800-108200

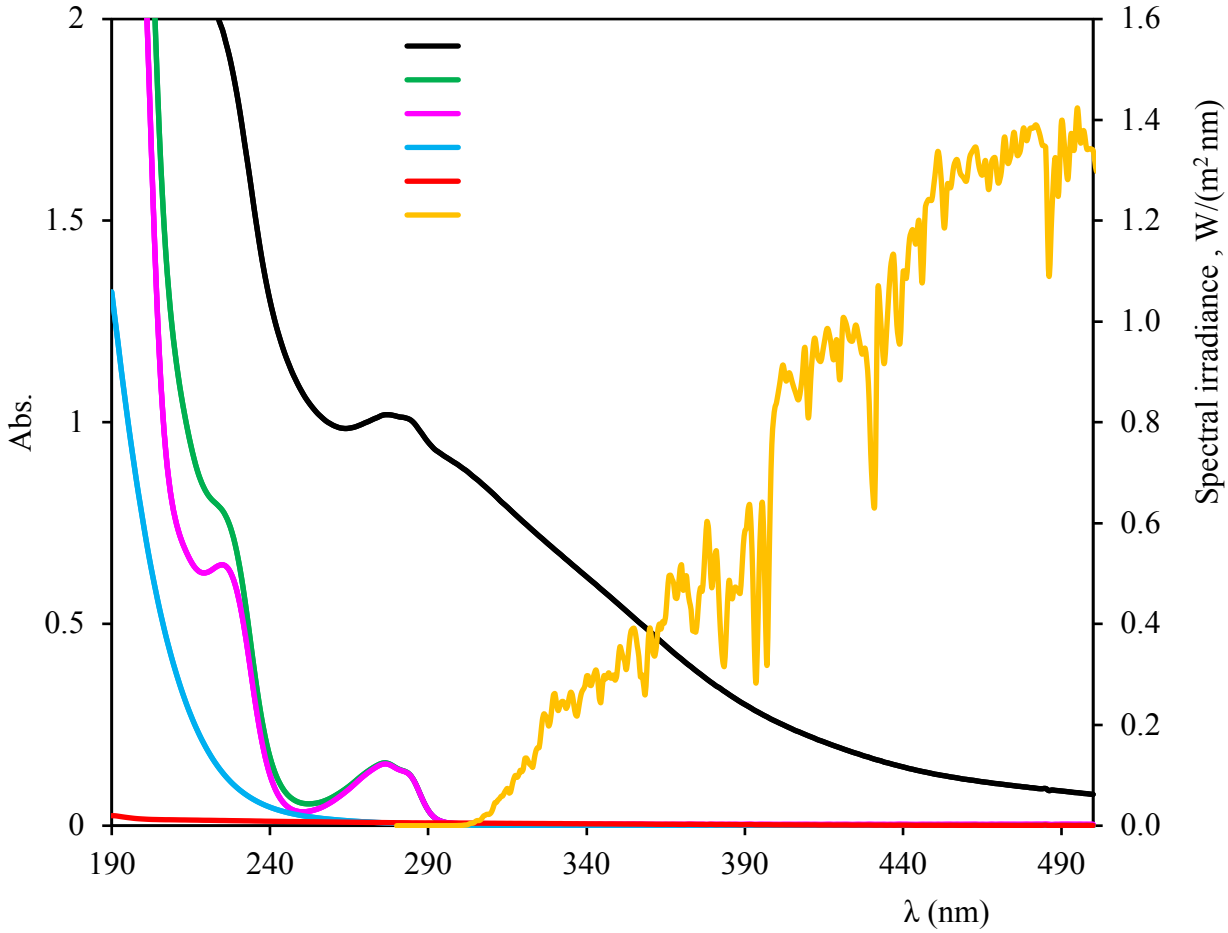

Fig. S1. Solar spectrum (ASTM) and absorption spectra of individual BPA, Fe^{2+}, $S_2O_8^{2-}$ solutions and their mixtures. [BPA] =43.8 μM, [$S_2O_8^{2-}$]=0.22 mM, [Fe^{2+}]= 71.4 μM .

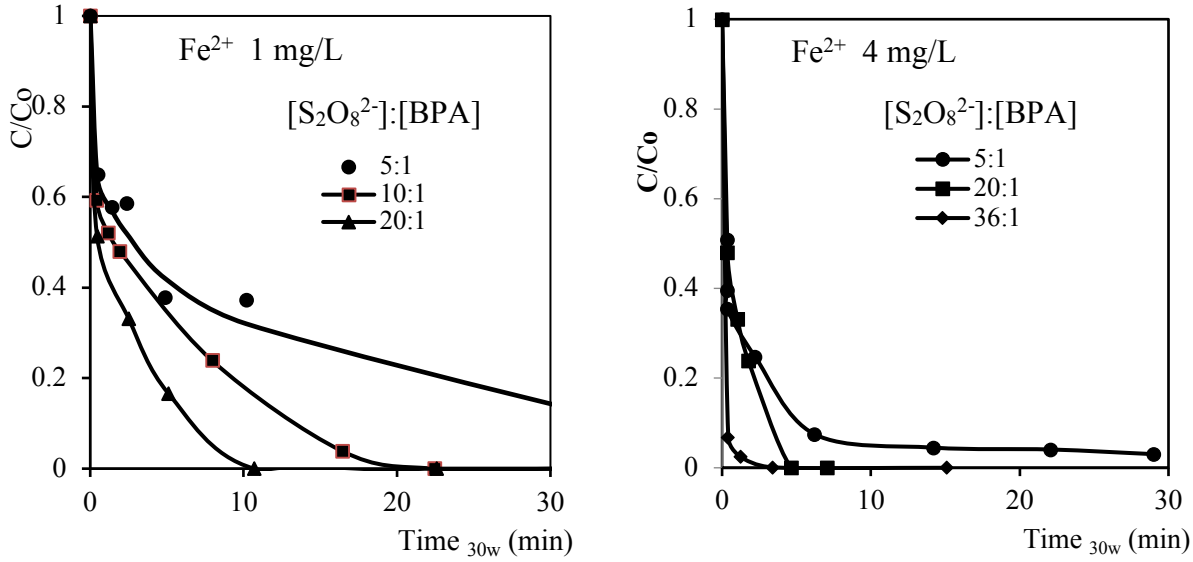

Fig. S2. – The effect of $S_2O_8^{2-}$ on BPA conversion. [BPA] =43.8 μM

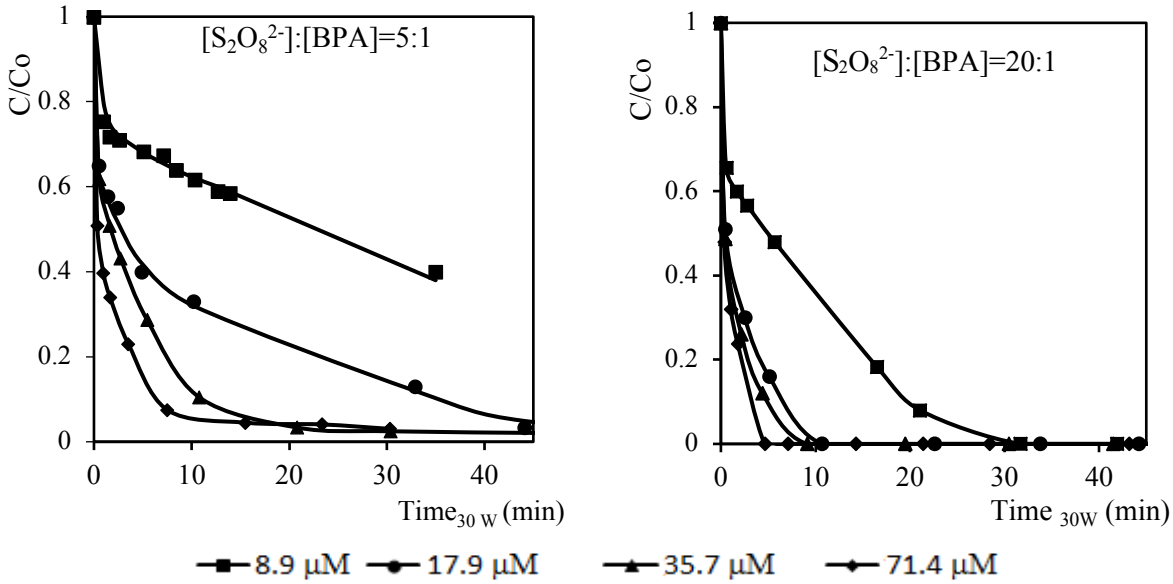

Fig. S3 - The effect of Fe^{2+} on BPA conversion. [BPA] =43.8 µM

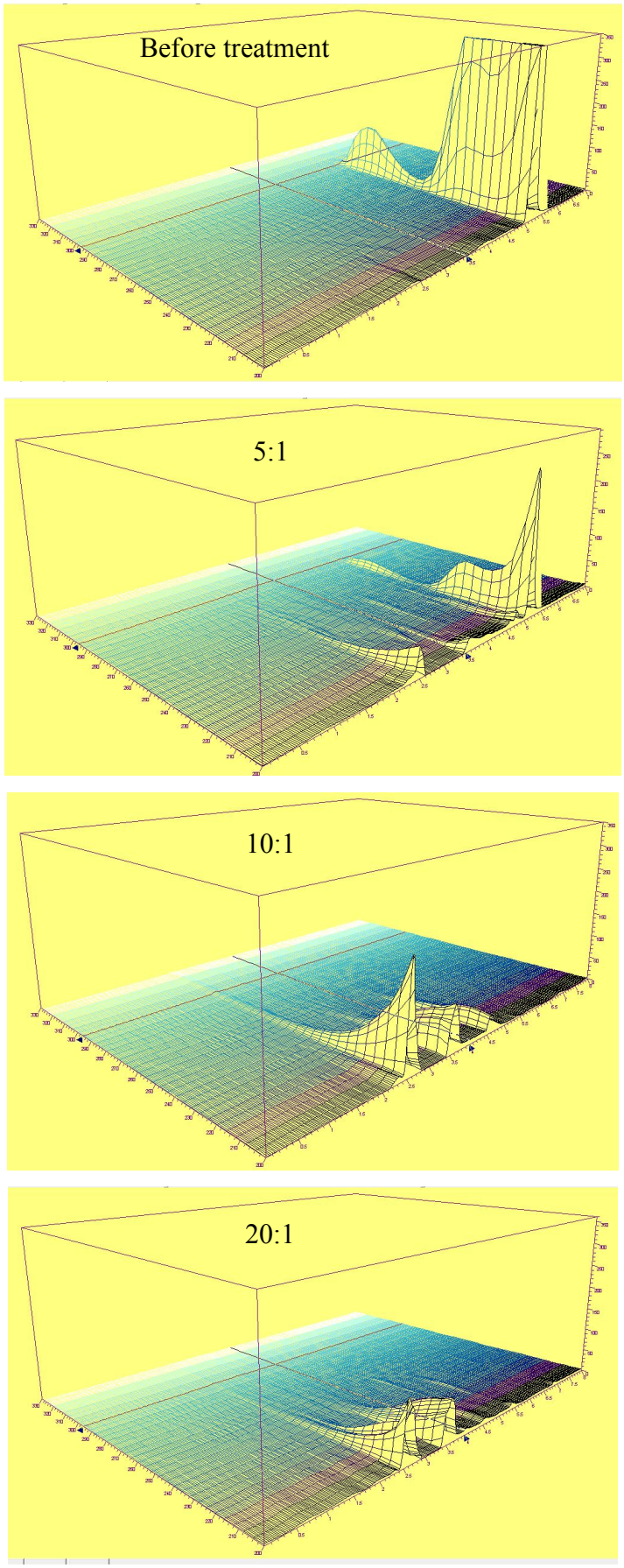

Fig. S4. - 3-D chromatograms of the test solutions before and after treatment at different molar ratios $[S_2O_8^{2-}]$:[BPA], [BPA] =43.8 μM, $[Fe^{2+}]$ = 17.85 μM. $Time_{30w}$=30 min.

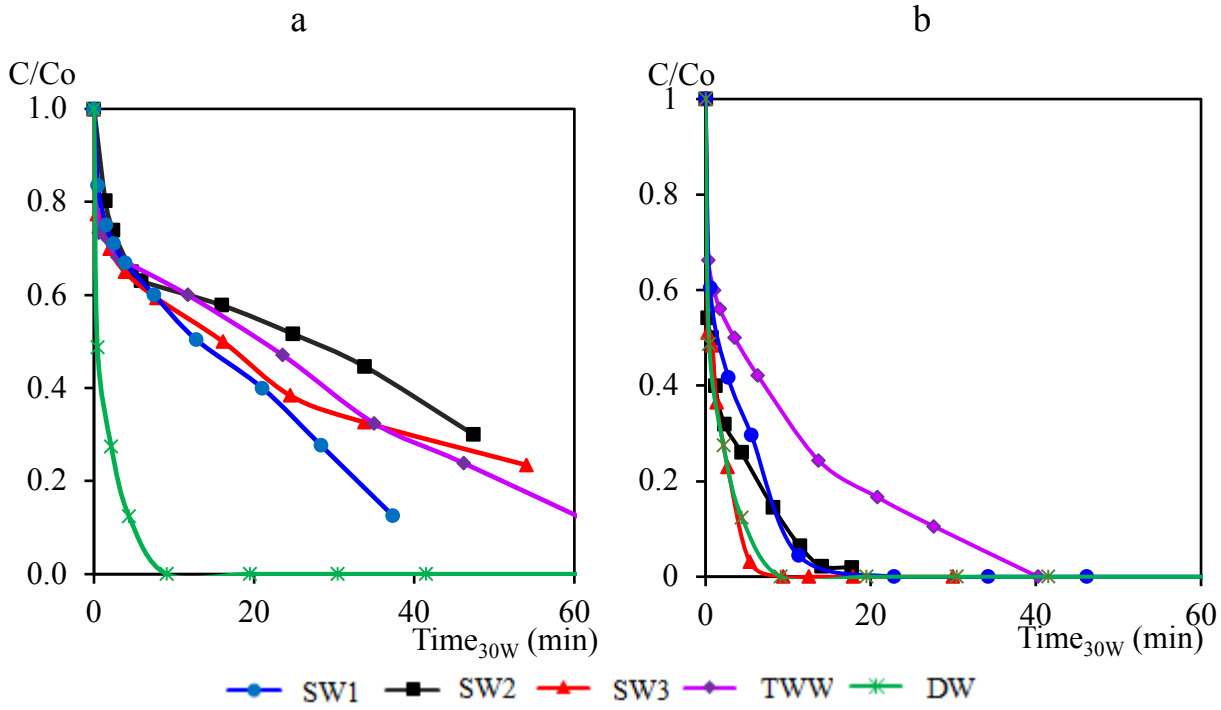

Fig. S5. Degradation of BPA by Solar / $S_2O_8^{2-}$/Fe^{2+} processes in aqueous matrices

a) non-adjusted pH; b) pH 4,5

[BPA] = 43.8 µM, [$S_2O_8^{2-}$]:[BPA] = 20:1, [Fe^{2+}] = 35.7 µM.

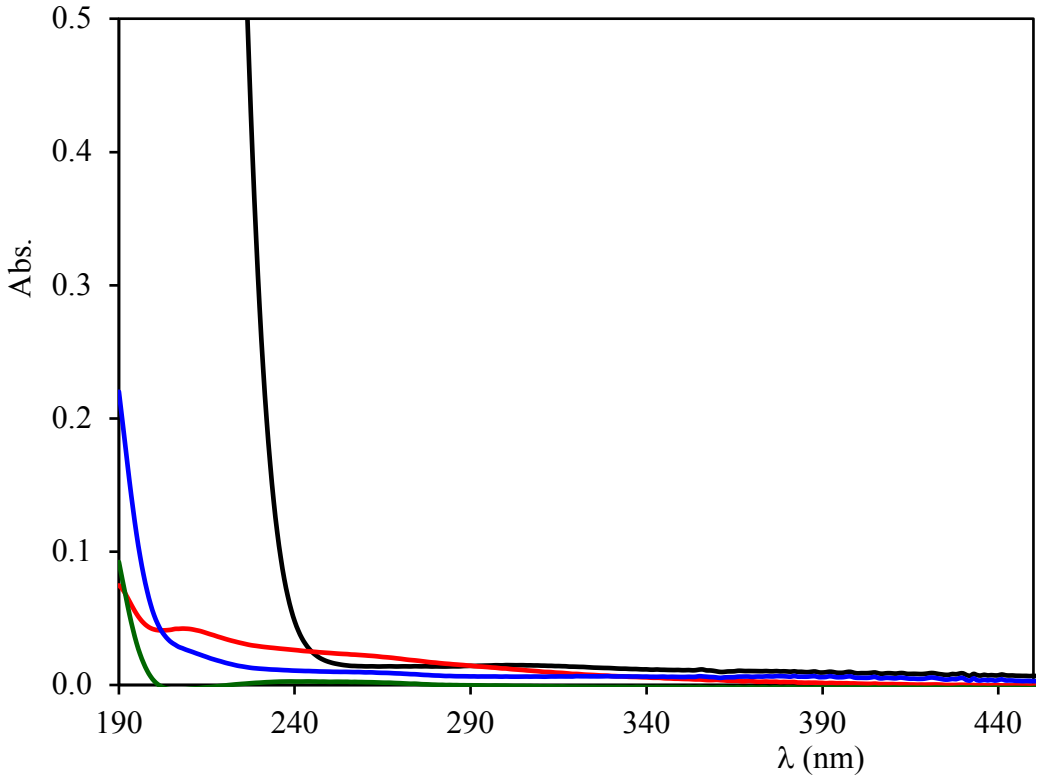

Fig. S6. Absorption spectra of water matrices used in the experiments